CORROSION INHIBITION BY *SHOREA ROBUSTA* (SAAL) BARK EXTRACT FOR MILD STEEL CORROSION IN 1 M H_2SO_4 SOLUTION

A DISSERTATION WORK SUBMITTED FOR THE PARTIAL FULFILLMENT OF THE REQUIREMENTS FOR THE MASTER OF SCIENCE DEGREE IN CHEMISTRY.

SUBMITTED BY:

Name: AJAY KUMAR BAJGAI

T.U. Examination Roll No.: 1579/2075

T.U. Registration No.:- 5-2-55-218-2014

SUBMITTED TO:

DEPARTMENT OF CHEMISTRY

AMRIT CAMPUS

INSTITUTE OF SCIENCE AND TECHNOLOGY

TRIBHUVAN UNIVERSITY, KATHMANDU, NEPAL

JUNE, 2022

BOARD OF EXAMINER AND CERTIFICATE OF APPROVAL

This dissertation entitled, "**Corrosion Inhibition by *Shorea robusta* (Saal) Bark Extract For Mild Steel Corrosion in 1 M H_2SO_4 Solution"** by, **Mr. Ajay Kumar Bajgai** under the supervision of **Assistant Professor Hari Bhakta Oil**, Department of Chemistry, Amrit Campus, Tribhuvan University, Kathmandu, Nepal, and under co-supervision of Asst. Prof. Dr. Deval Prasad Bhattarai, Department of Chemistry, Amrit Campus, Tribhuvan University, Kathmandu, Nepal, hereby submitted has been approved for partial fulfillment of the requirement for completion of his Master of Science (M.Sc.) Degree in Chemistry. This dissertation has not been submitted to any other university or institution previously for the award of a degree.

……

Supervisor

Asst. Prof. Hari Bhakta Oli

Department of Chemistry

Amrit Campus, TU, Kathmandu, Nepal

……

Co-Supervisor

Asst. Prof. Dr. Deval Prasad Bhattarai

Department of Chemistry

Amrit Campus, TU, Kathmandu, Nepal

……

External Examiner

Asst. Prof. Dr. Dipak Kumar Gupta

Department of Chemistry

Tri-Chandra Multiple Campus, Kathmandu, Nepal.

……

Internal Examiner

Asst. Prof. Sanjay Singh

Department of Chemistry

Amrit Campus, TU, Kathmandu Nepal

……

M.Sc. Chemistry Coordinator

Assoc. Prof. Dr. Bhusan Shakya

Department of chemistry

Amrit Campus, TU, Kathmandu, Nepal

……

Head of Department

Assoc. Prof. Kanchan Sharma

Department of Chemistry

Amrit Campus, TU, Kathmandu, Nepal

Date: June 16, 2022.

LETTER OF RECOMMENDATION

This is to recommend that the dissertation work entitled, "**Corrosion Inhibition by *Shorea robusta* (Saal) Bark Extract for Mild Steel Corrosion in 1 M H_2SO_4 Solution**" has been carried out by **Mr. Ajay Kumar Bajgai** as partial fulfillment for the requirements of Master of Science Degree in Chemistry. This is his original work and has been carried out under our guidance and supervision. To the best of our knowledge, this research work has not been submitted for any other degree at this institute.

…….

Supervisor

Asst. Prof. Hari Bhakta Oli

Department of Chemistry

Amrit Campus, TU,

Kathmandu, Nepal

…….

Co-Supervisor

Asst. Prof. Dr. Deval Prasad Bhattarai

Department of Chemistry

Amrit Campus, TU,

Kathmandu, Nepal

Date: June 10, 2022

DECLARATION

I, Ajay Kumar Bajgai, hereby declare that the work entitled "**Corrosion Inhibition by *Shorea robusta* (Saal) Bark Extract for Mild Steel Corrosion in 1 M H_2SO_4 Solution"** submitted to the Institute of Science and Technology Tribhuvan University as partial fulfillment for the requirements of Master of Science Degree in Chemistry has been done by myself and has not been submitted earlier in part or full in this or any other form to any other university/institute, here or elsewhere for the award of any degree.

……..

Ajay Kumar Bajgai

Roll No: 1579/2075

T.U. Registration No.:- 5-2-55-218-2014

Date: June 10, 2022.

ACKNOWLEDGMENTS

I would like to express my conscious deepest gratitude and sincere appreciation to my **supervisor, Assistant Professor Hari Bhakta Oli,** and **Co-Supervisor Assistant Professor Dr. Deval Prasad Bhattarai** for the continuous support of my research, for his patience, motivation, enthusiasm, and immense knowledge. His guidance helped me in all the time of research and writing of this thesis.

I would also like to thank **Associate Professor Kanchan Sharma,** Head of Department of chemistry, Amrit Campus, and **Associate Professor Dr. Bhusan Shakya,** Co-ordinator of M.Sc. program, Department of chemistry Amrit Campus as well as former M.Sc. Co-ordinator Professor Dr. Daman Raj Gautam, and former HOD Associate Professor Shree Dhar Gautam, Department of Chemistry Amrit Campus.

I am also thankful to the Central Department of Chemistry, Tribhuvan University for their kind help in Polarization measurement, and special thanks to Prof. Dr. Amar Prasad Yadav and Asst. Prof. Anju Kumari Das for helping me with polarization measurement and to take Optical Microscope images. I am also thankful to Kathmandu Valley College and Asst. Prof. Dr. Ram Lal Shrestha helping me for grinding the sample.

I am grateful to Province Planning Committee, Lumbini Province, for financial support (Research Grant Program 2078/79).

I am also grateful to Maniraj Budhathoki and Nanda Krishna Manandhar, who helped me provide all instruments. I accord my thanks to all teaching and non-teaching faculty members of the Chemistry Department, for giving kind support during the research work.

Finally, I have gratitude toward my family, friends, and the entire colleague who have direct or indirect involvement in the finalization of this research work.

Ajay Kumar Bajgai

Date: June 10, 2022.

Abstract

A novel corrosion inhibitor for mild steel (MS) corrosion has been extracted in methanol solvent from *Shorea robusta* bark. Qualitative chemical tests, VU, and FTIR measurements were carried out to confirm phytochemicals in the extract. The inhibition efficiency of extract has been studied by using weight loss and potentiodynamic polarization methods. The weight loss measurement has been adopted for the study of inhibitor concentration effect as well as variation of inhibition efficiency for time and temperature. Weight loss measurement reveals the maximum efficiency of 71.47% at ½ hours immersion time in 1000 ppm inhibitor concentration at 18 ^{o}C. The 1000 ppm inhibitor can work up to a temperature of 55 ^{o}C with 50% efficiency. The open-circuit potential (OCP) measurement reveals the extract as a mixed type of inhibitor. From the potentiodynamic polarization measurement results, the inhibition efficiency of the extract for MS was 93.73% and 75% in the 1000 ppm of inhibitor concentration for as-immersed and immersed conditions respectively. The adsorption isotherm and thermodynamic parameters support that the process is spontaneous and endothermic.

Keywords: *Shorea robusta, Extract, Green Inhibitors, Mild steel, Weight loss, Polarization*.

शोधसार

फलामको क्षयिकरण रोक्नका लागि सालको बोक्राबाट अवरोधक निकालियो । निष्काशीत अबरोधकको परिक्षण रसायनिक तथा प्रकाशिय वर्णपट अध्ययन विधिबाट गरियो । साथै त्यस अबरोधकमा भएको अवरोधकिय गुणको परिक्षण तौल मापन विधि र विद्युत रसायनिक विधि बाट गरियो । यसरि गरिएको अध्ययन अनुसार तेजाबजन्य पदार्थले फलाममा गराउने क्षयिकरणलाइ अबरोधकले ७१.४७ देखि ९३.७३ प्रतिशत सम्म रोकावट गरेको पाइयो साथै उक्त अवरोधकले ५५ डिग्री सेल्सीयस सम्म काम गर्ने देखियो ।

शब्द कुञ्जीका : *साल, निकाशी, अबरोधक, फलाम, तौल मापन*

LIST OF ABBREVATIONS

DW	:	Distilled Water
MS	:	Mild Steel
HER	:	Hydrogen Evolution Reaction
CP	:	Cathodic Protection
AP	:	Anodic Protection
OCP	:	Open Circuit Potential
OM	:	Optical Microscope
PVC	:	Polyvinly chloride
Θ	:	Fraction of Surface Coverage
C_{inh}	:	Corrosion Inhibitors
CR	:	Corrosion Rate
E_a	:	Activation Energy
ϕ_{corr}	:	Corrosion potential
FTIR	:	Fourier Transform Infrared Spectroscopy
I_{corr}	:	Corrosion current
mV	:	Milivolt
mV/s	:	Milivolt per second
ppm	:	Parts per million
SCE	:	Saturated Calomel Electrode
UV	:	UltraViolet

LIST OF TABLES

LIST OF FIGURES

TABLE OF CONTENTS

CHAPTER - 1
INTRODUCTION

1.1 Corrosion Introduction

Corrosion is a naturally occurring irreversible and complex phenomenon that converts a refined metal into a chemically more stable form such as oxides, hydrides, or sulfides. It is the gradual destruction of materials by chemical and/or electrochemical reactions with their environment. Corrosion can occur due to interaction with many matters like air, water, dirt, bacteria, acids, bases as well as many other organic and inorganic compounds (Gupta et al., 2020). Corrosion is common in almost all kinds of materials (Metals, Alloys, Ceramics, Polymers, Intermetallic compounds, Glass, Leathers, Woods, etc.) (Brycki et al., 2018) but it rapidly happened in metals and alloys because generally pure metals and most of the metallic alloys are chemically unstable thereby react rapidly with the constituents of the surrounding environment by chemically or/and electrochemically. Corrosion is the spontaneous process that drives the materials to their lowest possible energy states i.e. change in free energy is negative (ΔG^o = -ve). That means a more negative change in the value of standard Gibb's free energy change ΔG^o leads to a higher corrosion rate (Verma et al., 2018). Electrochemically corrosion takes place through the process of cathodic and anodic reactions (Brycki et al., 2018).

- In the anodic reaction metal (M) gets oxidized with the liberation of the electron as,

$$M \rightarrow M^{n+} + ne^- \quad \ldots 1$$

- In the cathodic reaction reduction of metal/alloy takes place at the surface of the metal.

Reduction of metal $M^{n+} + ae^- \rightarrow M^{(n-a)}$ … 2

Where 'n' be the number of electrons that are involved in the reaction.

Reduction based on the surrounding environment is shown as,

a. Hydrogen evolution reaction

From Acid: $2H^+ + 2e^- \rightarrow H_2 \uparrow$ … 3

From Water : $2H_2O + 2e^- \rightarrow H_2 \uparrow + 2OH^-$ … 4

b. Reduction of Oxygen

In Acidic solution: $O_2 + 4H^+ + 4e^- \rightarrow 2H_2O$ … 5

In Basic/Neutral solution : $\frac{1}{2}O_2 + H_2O + 2e^- \rightarrow 2OH^-$ … 6

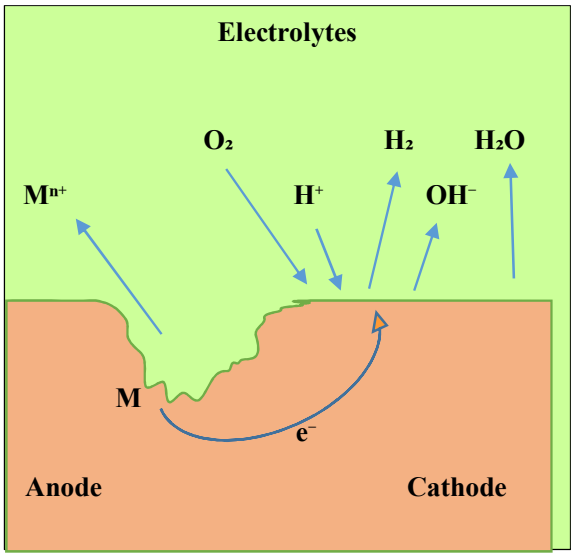

Figure 1: Scheme of electrochemical corrosion

Mild steel is the widely used iron-carbon alloy that may also contain Manganese, Silicon, Sulphur, Phosphorous, and Copper. For the references, the mild steel sample A516 grade 60 is composed of 0.21–0.27% C, 0.13–0.45% Mn, 0.79–1.30% Si, 0.035% P, 0.035% S, and the rest of Fe (Chapagain et al., 2022; Ugi & Magu, 2018) Mechanical properties like maximum stress, yield stress, elongation, corrosion resistance, etc. of the mild steel all are dependent on the ruling, section composition, and manufacturing process.

In modern technology, modern civilization and modern engineering can't survive without steel (Liu et al., 2021). It has great industrial applications like manufacturing oil tanks, pipelines, gas cylinders, heat exchangers, microchips, and weighing machines as well as in structural applications and machinery. Such great application is due to its better mechanical properties, cost-effective, easy availability, weldability, malleable even when cold, high resistance to breakage, ease of fabrication, gives a nice finish, and is polishable (Peter & Sharma, 2017). Thus corrosion is the unintentional attack of the metal and exists everywhere, destruct almost all constructions and there is no industry or house where it does not affect hence corrosion scientists and engineers should understand the cause of corrosion and try to fight against this problem (Revie, 2008). From literature, it is found that corrosion destroys one-quarter of the world's steel production and approximately 3-4.5% of the Gross National Products (GNP) of an industrialized country is lost due to corrosion. The annual direct cost of corrosion for highway bridges is estimated to be $ 13.6

billion all over the world (Phulara, 2019; Rana, Joshi, & Bhattarai, 2017; Sivakumar & Srikanth, 2017; Thapa, Gupta, & Yadav, 2019). Thus it is necessary to stop the corrosion rate however it is challenging work for corrosion scientists and engineers.

1.2 Corrosion Protection

Corrosion is an irreversible and spontaneous process so it can't eliminate but prevention can be applied to more or less extent for the prevention from corrosion by using the appropriate method. Some of the corrosion protection methods are given.

1.2.1 Microstructure Design

In the recent year a novel conception of alloying free "plain material" given by K. Lu et al., can be significantly adopted by microstructure design across the different scales without changing the chemical composition and can minimize the corrosion rate in various corrosive environments (Liu et al., 2021) but there are various other corrosive environments where microstructure designation and selection of material can't address the whole corrosion problem for a long period.

1.2.2 Coating

The coating is the process of isolation of the metal from the corrosive environment that decreases its resistance to corrosive degradation. In the process, thin layers of a covering substance are deposited or applied on a surface of any metal or object to form protective barriers against deterioration of the surface. A protective coating may be metallic (galvanized steel or tin-plates steel) or non-metallic (organic or inorganic). The most important non-metallic coating are polymers made from epoxides, polyesters, polyurethanes, resins, phenolic polymers, polyacrylates, polyphosphates, nitrites, and graphene, hybrid based on graphene oxide, silica-titania hybrid, tungstates, etc. These coatings include an inner primer layer loaded with anti-corrosion pigments, and a wide variety of these exists in the market. Organic extract and polymer coating are introduced into the metal surface that shields the corrosion of metal (Brycki et al., 2018; Morozov et al., 2019; Zhang et al., 2019). A good coating should meet the characteristics and requirements of having a high degree of adhesion to the substrate, high resistance to the flow of electrons, sufficient thickness, and a long life even at a low cost.

1.2.3 Galvanization

Galvanization is the surface treatment that allows for protecting materials from corrosion by metallic coating on the iron/steel surface (Berto & Fergani, 2017). The metallic coating can be carried by electroplating more reactive metals such as Zinc, Aluminum, Calcium, Sodium, Magnesium, etc. than Iron, but the galvanization process is carried out only by using Zinc. Literature shows that the galvanizing industries are suffering from the high consumption of Zinc and increasing costs due to excessive coating of Zinc. The US reported that 87% of the total consumption of Zinc (about 517,000t) was used for the galvanization process only (Valet, Burkert, Ebell, & Babutzka, 2021). This coating causes difficulty in the reuse and recycling of material as well as it is not suitable for a time in acidic media due to hydrogen evolution reactions (HER).

1.2.4 Anodic protection

Anodic protection (AP) is the method or technique to control the corrosion of a metal/alloy surface by making it an anode to an inert cathode of an electrochemical cell and controlling the electrode potential as metal gets passivate. Anodic inhibitors act usually by forming a protective oxide film on the surface of the metal (Ahmad, 2006). The most common anodic protection is passivation in which the metal surface is passivated by the deposition of an oxide film. The anodic protection is most widely applied to protect equipment used to store and handle sulphuric acid (Revie, 2008) but it is unable to form a stable continuous protective film on the metal to be protected.

1.2.5 Cathodic protection

Cathodic protection (CP) is a technique that is used to control the corrosion of metal by making it the cathode of an electrochemical cell and its potential is driven negatively to a point where the metal is immune to corrosion. The reaction at the surface of the material will be hydrogen evolution and/or oxygen reduction. The mechanism can be understood by the mechanism of following the reaction (Gladkikh et al., 2019).

$$H_2O + O_2 + 4\,e \rightarrow 4\,OH^- \qquad \ldots 7$$

$$2\,H^+ + 2\,e \leftrightarrow H_2\uparrow \qquad \ldots 8$$

In the first reaction, the cathode gets reduced by the diffusion of oxygen to the metal/electrode interface. If another metal such as magnesium and zinc, is added to

the metal/electrolyte system, it would react with the hydroxyl ion and precipitate insoluble compounds which would turn stifle the cathodic sites on the metal. In the second reaction hydrogen evolution reaction (Garcia-Cabezon, Salvo-Comino, Garcia-Hernandez, Rodriguez-Mendez, & Martin-Pedrosa, 2020) takes place by the process of adsorption of hydrogen ions on the metal surface and reduction to atomic hydrogen by accepting electron released by metal atom (Ahmad, 2006). Mainly there are two types of CP, one is the sacrificial anode which is most commonly used & called galvanic protection also and another is impressed current CP in which an electric power rectifier from an external source is opposed to the discharge of corrosion from an anodic area of the structure (Oghli, Akhbari, Kalaki, & Eskandarzade, 2020; Wang, Xu, Xu, Jiang, & Ma, 2020). Cathodic protection can be an effective method of preventing stress corrosion cracking and much useful to protect metal corrosion for underground structures but it can't be applied to protect from atmospheric corrosion and can't be applied in a poorly conductive environment (Zarras & Stenger-Smith, 2014). Cathodic protection can be applied as an effective method of preventing stress corrosion, pitting corrosion, stress-corrosion cracking, intergranular corrosion, and corrosion fatigue of most metals such as steel, copper, lead, brass, magnesium, aluminum, etc. as well as in almost aqueous media but it can't applicable in the water line and hydrogen cracking of such steels in acidic media (Revie, 2008).

1.2.6 Use of inhibitors

One of the common approaches to control such corrosion of mild steel/metals is to add small amounts of inhibitors to the production fluid. An inhibitor is a chemical substance/impurity that in addition to a small amount to the corrosive environment decreases the corrosion rate of the materials by replacing the water molecule from the neighborhoods of the metallic surface then its species can interact with anodic and cathodic active sites through the adsorption phenomena (Al-Shihry, Sayed, & Abd El-lateef, 2020). The effectiveness of inhibitors is partly dependent on the metals/alloys to be protected as well as the severity of the environment and they reduce the rate of corrosion by reducing either the anodic or cathodic reaction or a combination of both. Inhibitors are the synthetic chemical compounds or phytochemicals that when added to the acid solutions reduce corrosion. Inhibitor molecules are electron-rich species that act as active centers for the adsorption process on the metal surface.

The efficiency of the inhibitor can be expressed as,

$$E_{\text{inh}} = \frac{CR_0 - CR_i}{CR_0} \times 100 \qquad \ldots 9$$

Where $\mathbf{E}_{\text{inh}}$ = efficiency of corrosion inhibitor

CR_0 = corrosion rate with zero inhibitor

CR_i = corrosion rate in the presence of an inhibitor

The quantity of inhibitors required for a fluid to be inhibited can be obtained by the relationship: (Rana et al., 2017).

$$Q_{inh} = \frac{V_{fluid}}{1.0 \times 10^6} \times C_{inh}\ (ppm) \qquad \ldots 10$$

Where Q_{inh} = quantity of inhibitor in Kg

V_{fluid} = volume of fluid to be inhibited

C_{inh} = inhibitor concentration in ppm

Several methods like inorganic, organic, and polymer coating are applied for the prevention of corrosion.

a. Polymer Inhibitor

Polymeric materials have gained popularity as corrosion inhibitors for metals and alloys in recent years due to their superior corrosion inhibition properties when compared to simple organic species (Al-Shihry et al., 2020). Polymers are used in a variety of industries, including biomedicine, sensors, rechargeable batteries, catalysis, and microbial fuel cells, to name a few. The length of the carbon chain and the polymers' multiple adsorption sites can prevent a substantial portion of the metal contact from forming. Polypyrrole (PPy), poly (3,4-ethylene dioxythiophene (PEDOT)), and polyaniline (Gupta et al., 2020) are all examples of polypyrrole (Garcia-Cabezon et al., 2020) Polyethylene glycol, polyvinyl pyrrolidone (PVP), polyvinyl-benzyl trimethyl ammonium chloride (PVBTMA), polyvinyl alcohol (PVA), and poly(- diphenylamine (Al-Shihry et al., 2020) are the most common polymers used for corrosion protection of active metals like aluminum, copper, nickel, titanium, iron, and steel, as well as (Garcia-Cabezon et al., 2020). Polymer liners are used to mitigate internal corrosion in natural gas pipelines because they reduce the rate of corrosion by reducing the reactive gas flux to the pipeline's internal surface (Ali, Magee, & Hsieh, 2020).

b. Inorganic inhibitors

There are many inorganic compounds, and their addition to anodic-cathodic zones causes the electrochemical response to be suppressed. Inorganic inhibitors are divided into two categories: anodic and cathodic inhibitors. Chromates, nitrites, molybdates, tungstates, silicates, and phosphates are used as anodic inhibitors that regulate the rate of oxidation reactions by moving the metal's mixed corrosion potential to the noble direction. Many structural metals are well-protected by these oxidative-type inhibitors across a wide pH range. However, because chromates are known to be carcinogenic and poisonous, they should be replaced with more ecologically friendly materials. Tungstates and molybdates are similarly effective inhibitors, but they are less hazardous than chromates since their chemical structure is comparable to that of chromate. When chromates are ineffective, they are effective inhibitors (Gladkikh et al., 2019; Makhlouf & Botello, 2018; Sayin & Karakaş, 2013). Because of their ability to passivate the metal surface, nitrates and chromates are known as passivating inhibitors.

c. Organic Inhibitor

For the adsorption process on the metal surface, many organic compounds contain heteroatoms that are rich in electrons and activity centers. These electrons can be transferred to the metal surface that inhibiting metal corrosion. And this type of adsorption leads anodic and cathodic reactions to be blocked indirectly by slowing the diffusion of reactants to the metal's surface and forming a protective barrier coating. Most organic inhibitors adsorbed on metal surfaces when water molecules were replaced, according to known data. At room temperature, most of the inhibitors adsorb to the metal surface via physical and chemical adsorption. These are also known as adsorption site blockers or side blocking species. Based on their chemical structure and physical attributes such as electron density at the donor atom, p-orbital character, and electronic structure of the molecule (i.e. reverse order of the electronegativity of atoms), the inhibition efficiency should follow the sequence ONSP (Sivakumar & Srikanth, 2017; Thapa et al., 2019; Verma et al., 2018). Previously, the inhibitory efficiency increased as the carbon chain length increased, which was attributed to the decreasing solubility in an aqueous solution as the carbon chain length increased. The standard adsorption free energy (ΔG_{ads}) can be used to investigate the different types of adsorption (Brycki et al., 2018).

d. Synthetic inhibitors

The most effective corrosion inhibitors are organic molecules with heteroatoms such as O, N, S, P, X, and –bonds. Because of their inherent stability and cost-effectiveness, polymers have recently attracted a lot of attention as corrosion inhibitors. Furthermore, they form complexes with metal ions through their functional groups, and these complexes occupy a significant surface area on the metal surface, blanketing the surface and shielding the metals from corrosive substances present in the solution (Umoren, Ogbobe, Igwe, & Ebenso, 2008). Some research groups have investigated the use of polymers as corrosion inhibitors of metals in aggressive media. Polymers such as polyvinyl alcohol, polyethylene glycol, polyvinyl pyridine, polyvinyl pyridine, polyvinyl pyrrolidine, polyvinylpyrrolidone (PVP) polyethyleneimine, polyacrylic acid, polyaniline, polyacrylamide, and polyvinyl imidazole have reported. Because of the presence of the -C=N- group (imines), N, and O atoms in the molecule, Schiff bases are considered strong corrosion inhibitors for a variety of metal/alloy surfaces in acidic conditions (Arshad et al., 2019). But most organic compounds are toxic as well the synthesis of organic polymeric compounds is difficult and expensive, their synthesis process pollutes the environment on a larger scale and is non-biodegradable so their uses are limited.

e. Green inhibitors

Although synthetic organic compounds inhibit the corrosion of mild steel, show toxicity to human health, and production of unwanted several side products in their synthesis process cause diverse effect in the surrounding environment so there must be the search for a kind of inhibitor they are biodegradable, eco-friendly, easily available, biodegradable, do not contain heavy metals or other toxic compounds and ecologically acceptable as alternatives of minimal health environmental risk is termed as green corrosion inhibitors (Li, Zhang, & Wu, 2018). Plant extracts of natural products are commonly used as green corrosion inhibitors. Several chemical molecules with polar atoms, such as O, N, P, and S, can be found in these extracts. Through these polar atoms, they are adsorbed onto the metal surface, forming protective coatings. These compounds' adsorptions follow a variety of adsorption isotherms. Adsorption appears to be primarily influenced by the inhibitor group's physicochemical features, such as functional group, electron density at the donor atom, orbital character, and electronic structure Plant extract of natural products are

commonly used as green corrosion inhibitors. Several chemical molecules with polar atoms, such as O, N, P, and S, can be found in these extracts. Through these polar atoms, they are adsorbed onto the metal surface, forming protective coatings. These compounds' adsorptions follow a variety of adsorption isotherms. Adsorption appears to be primarily influenced by the inhibitor group's physicochemical features, such as functional group, electron density at the donor atom, orbital character, and electronic structure (Bhattacharjee, Islam, & Sciences, 2015). High molecular weight bulky hetero compounds like Alkaloid, Flavonoid, Imidazole, Glucose, Aminoacids, Sarasapogenin, quinolone derivatives, thiourea derivatives, thiosemicarbazide, thiocyanates, saponins, and tannins, etc. (Finšgar & Jackson, 2014; Mendes, da Silva, & Rocha, 2012; Rahim, Hassan, & Khalil, 1997; Salada, Balala, & Vasquez, 2015) are used for the corrosion inhibition process.

1.2.7 Significance of green inhibitor

Nepal is rich with widespread biodiversity, various types of flora and fauna flourish are available in the Himalayan to the Terai region which inspires us the use natural products as a corrosion inhibitor, which is ecofriendly and greener (Gupta et al., 2020). Green corrosion inhibitors are non-toxic, low-cost, readily available, and renewable sources of materials as compared with organic chemicals as corrosion inhibitors (Dariva & Galio, 2014). So the use of biodegradable organic compounds as inhibitors could be the best way of protecting metallic material against corrosion damage.

1.3 Mechanism of corrosion inhibition

It is known that inhibitor molecules are adsorbed on the material surface either physically or chemically and they release the electron for metal during corrosion and reduce the corrosion rate. During the process when a material is subjected to a corrosive environment while containing inhibitor molecules, the inhibitor molecules become adsorbed on the material's surface and act as a barrier to the corrosive environment. Adsorption mechanisms are usually addressed using various adsorption isotherms and metal inhibition by organic substances as a result of (molecules and/or ions) adsorption at a solid surface (Faraj & Khan, 2015).

Physisorption occurs when inhibitors are adsorbed by electrostatic interaction between inhibitor ions or dipoles and an electrically charged metal surface. Coordinate bonds are generated in chemisorption when electrons are transferred from inhibitors serving as ligands to the metal's empty orbital. The polar group of inhibitors that act as the anchoring group displaces the water molecules adsorbed on the material surface in both adsorptions, and the non-polar end is directed vertically to the metal surface, repelling the corrosive species (Revie, 2008). The general mechanism of corrosion inhibition is shown in the figure below.

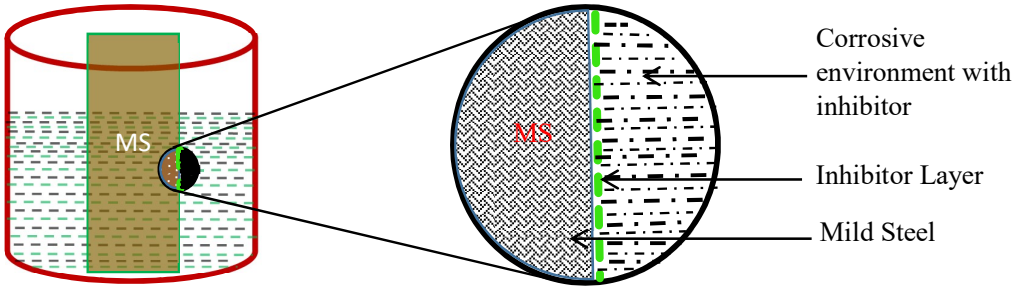

Figure 2: Scheme of corrosion inhibition mechanism.

1.4 Objectives of the study

1.4.1 General objective

The main objectives of the present work are to prepare *Shorea robusta* bark extract and study its anticorrosion activity.

1.4.2 Specific objectives

1. Preparation of *Shorea robusta* barks extracts in methanol.
2. Isolation of Alkaloid and Polyphenol from the extract.
3. Study the inhibition efficiency using the weight loss and potentiodynamic polarization method.
4. Study the various thermodynamic parameters and examine the Langmuir and Freundlich adsorption isotherms.

1.5 Rationale of the study

It is reported that approximately 3-4.5% of the GNP of an industrialized country is lost due to corrosion. The annual direct cost of corrosion for highway bridges is estimated to be $ 13.6 billion all over the world (Sivakumar & Srikanth, 2017; Thapa et al., 2019; Verma et al., 2018). There is about 4.3% of GDP loss due to corrosion in our country Nepal, among which 30-35% can be saved through corrosion protection methods (Karki, 2021). After completion of this research, one of the green corrosion inhibitors will be discovered. The development of such an inhibitor will uplift the country's economy in two ways: i) reducing the cost of corrosion, and ii) exporting the inhibitor extracted from *Shorea robusta*. So, this research is relevant to the national priority, for the economic growth of the country.

CHAPTER – 2
LITERATURE REVIEW

2.1 Review of Work

Thapa B. et al., (2019) have reported the bark extract of *Euphorbia royleana* as a green corrosion inhibitor in 1M HCl with significant inhibition using the weight loss method and potential measurement. The results show that the bark extract of *Euphorbia royleana* is an effective anti-corrosion inhibitor of mild steel in acidic media. The corrosion rate decreases with the time of immersion. The weight loss experiment shows that the loss in weight decreases with the time of immersion and inhibition efficiency increases with the concentration of extract. It was observed that maximum inhibition efficiency is 99.60% in 100% concentration of extract. A potential measurement study shows that bark extracts act as a mixed type of inhibitor i.e. inhibits both anodically as well as cathodically. FTIR analysis suggested that the adsorption takes place due to the presence of functional groups O-H, C≡N, and C=O group (Sivakumar & Srikanth, 2017; Thapa et al., 2019; Verma et al., 2018).

Aralu C. C., (2021) used the weight loss method and found *Gongronema latifolium* would be a low-cost green inhibitor for mild steel. As the temperature rose, the percentage of inhibition decreased, whereas an increase in inhibitor concentration increased inhibition efficiency. According to the results, the percentage inhibition efficiencies of the methanol extract of Gongronema latifolium ranged from 59.06 to 81.69 percent. In contrast to the Freundlich and El-Awardy adsorption models, mild steel corrosion inhibition showed an excellent fit to the Langmuir model. The evaluation of thermodynamic parameters such as Ea, Q_{ads}, and G_{ads} revealed that physisorption was the mechanism by which the mild steel corrosion caused by the methanol extract of Gongronema latifolium was inhibited. The findings of this study suggested that methanol had a high potential (Aralu, Chukwuemeka-Okorie, & Akpomie, 2021).

Shrestha P. R. et al., (2019) have studied methanol extract of barks of *Lantana camara* in 1 M hydrochloric acid as a corrosion inhibitor. Methanolic extract of barks of *Lantana camara* in 1 M hydrochloric acid was tested as a corrosion inhibitor on mild steel using the potentiodynamic polarization technique. The corrosion inhibition efficiency of extract varied with the concentration of extract and immersion of time.

The inhibition was found to increase with an increase in the concentration of the extract. The polarization behavior of mild steel revealed that maximum inhibition efficiency is 97.33 % and 89.93 % respectively in the 1000 and 200 ppm concentration of the inhibitor. The results showed that the extract of the barks of *Lantana camara* served as a mixed-type inhibitor (Shrestha et al., 2019).

Berrissoul A., et al. (2020) evaluate the *Lavandula mairei* extract as a green inhibitor for mild steel corrosion in 1 M HCl solution and they found the Inhibition efficiency up to 92% at temperature 303K (Berrissoul et al., 2020). The corrosion inhibition properties of *Eucalyptus globulus* extract in 0.1M HCl were studied by Gupta D.K. et al. (2020) and found very significant inhibition efficiency. Corrosion inhibition of MS in 0.1M HCl was studied in the absence and presence of various concentrations of the acidic extract of EG barks using the weight loss method and open circuit potential (OCP) measurement. The results showed an increase in corrosion inhibition with increasing concentration of the extract. The inhibition efficiency of 100% EG extract was approximately 98.0% after 24 hours of immersion in the acidic solution. FTIR spectrum showed the presence of compounds containing oxygen and nitrogen functional groups responsible for forming barrier layers on the MS surface. Open circuit potential (OCP) measurements showed that the EG extract acts as a mixed-type inhibitor (Gupta et al., 2020).

Rana M. et al., (2017) studied the corrosion inhibition effect of *Areca catechu*, *Laurus nobilis,* and *Catharanthus roseus* plant extracts on mild steel was investigated in 0.5 M NaCl solution in the open air at 28 ± 1 °C using immersion tests, inhibition mechanism, and corrosion potential measurements. The corrosion rate of the steel was decreased with increasing the concentration of the extracts up to 2000 ppm. *Catharanthus roseus* plant extract was found to be the most efficient inhibitor among the three extracts used in this study. Adsorption of all three plant extracts on the surface of the mild steel obeyed both Langmuir and Temkin adsorption isotherms. *Areca catechu* and *Catharanthus roseus* plant extracts acted as an anodic type corrosion inhibitor, while *Laurus nobilis* extract acted as a mixed type inhibitor based on the potential measurement in the simulated aggressive environment (Rana, Joshi, & Bhattarai, 2017).

Using gravimetric and spectroscopic methods examined the inhibitive efficiency of Green Tea (GTE) and Black Tea (BTE) extracts on mild steel in an acidic environment. The efficiency of both extracts to inhibition (Yahaya, Aroyeun,

Ogunwolu, Jayeola, & Igbinadolor, 2017) efficiency increases as the concentration of extract increases and decreases as the temperature rises. At 0.25 g/L inhibitor concentration, maximum inhibition efficiency for GTE and BTE has been found as 83 and 81.7 %, respectively. The adsorption mechanism was spontaneous, exothermic, and physisorption, and it followed the Langmuir isotherm. FTIR spectra revealed the development of the active compound-Fe complex.

Nanna et al., (2014) showed that different concentrations of *Gmelina arborea* bark extract inhibit mild steel corrosion in an acidic solution of 1.0 M HCl at room temperature. After 40 hours of exposure, the corrosion rate of mild steel was reduced from around 0.6 mm/yr to as low as 0.04 mm/yr, resulting in high inhibition efficiency values of 94% to an optimum value of about 96%. Langmuir and Temkin's isotherms indicated a mixed adsorption mechanism, and negative values of Gibb's free energy of adsorption indicate the process is spontaneity (Nnanna, Uchendu, Nwosu, Ihekoronye, & Eti, 2014). Hari Kumar and Karthikeyan used weight loss, potentiodynamic polarization, electrochemical impedance spectroscopy, hydrogen permeation, and diffuse reflectance spectroscopic techniques to investigate the corrosion inhibition of mild steel in 1M Sulphuric acid employing Amoxicillin as an inhibitor. As the concentration of the inhibitor rises, so does the efficiency of the inhibition. There are no notable changes in surface morphology, according to diffuse reflectance spectra and SEM pictures. Inhibitors behave as mixed-type inhibitors, according to potentiodynamic polarization experiments, and their adsorption on mild steel surfaces follows the Langmuir adsorption isotherm (Kumar & Karthikeyan, 2013). Muthukrishnan et al., (2014) used *Hyptis suaveolens* leaves extract to inhibit mild steel corrosion in H2SO4 and found that inhibition efficiency improved as extract concentration increased, with a maximum inhibition efficiency of 95% and the extract acting as a mixed type inhibitor (Muthukrishnan, Jeyaprabha, & Prakash, 2014).

Mathur et al., (2014) used the mass loss method to investigate mild steel corrosion in various concentrations of hydrochloric acid and sulphuric acid in the absence and presence of extract from the seeds of *Pennisetum glaucum*. Corrosion inhibition was shown to rise proportionately to the extract concentration. The seed extract of the plant *Pennisetum glaucum* has been discovered to be beneficial and has a good corrosion inhibition efficacy (Mathur & Chhipa, 2014).

Research has not been limited up to this; the number of plant extracts has been reported as green inhibitors. Extracts of *Areca catechu*, *Laurus nobilis,* and *Catharanthus roseus* (Rana M. et al., 2017), *Ziziphus joazeiro* Stem Bark Extract (Mauro et al., 2021), *Amorphophallus paeoniifolius leaves* extract (Guruprasad & Sachin, 2021)*, Allamanda cathartica* leaves extract (Banu, Farzana, & Ahamed, 2021), walnut fruit green husk extract (Shahmoradi et al., 2021), and many more have been reported as green inhibitors for mild steel in acidic medium. Such inhibitors are reported with good inhibition efficiency only below 45 °C. Plant abundance, extract with higher inhibition efficiency, and good inhibition at higher temperatures are still to be considered.

2.2 Selection of Plant Material and Research Gap

Taxonomy

Kingdom	Plantae
Subkingdom	Viridiplantae
Infrakingdom	Streptophyta
Superdivision	Embryophyta
Division	Tracheophyta
Subdivision	Spermatophytina
Class	Magnoliopsida
Superorder	Rosane
Order	Malvales
Family	Dipterocarpaceae
Genus	Shorea
Species	*robusta*
Common Names	Saal tree

Figure 3 : Shorea robusta.

Shorea robusta of the family Dipterocarpaceae is an abundant plant in Nepal. It is found in the Terai region to 1500 m but common up to 1000 m. It occurs mostly in Terai, Siwalik, and low land hilly areas. It is called the Sal tree in Nepali. Sal tree is a

moderate to slow-growing tree that can attain heights of 30 to 35 meters and a trunk diameter of up to 2-2.5 meters. Some deciduous trees are up to 50 m tall and with a diameter of 5 m (Baral et al., 2020; Soni, Dixit, Irchhaiya, & Singh, 2013). It consists of thick bark about 8-12mm that is used for medicinal purposes traditionally, the plant is used for dysentery, Ulcers, Jaundice, wounds, gonorrhea, and leprosy. The bark is used as astringent, acrid, cooling, antihelmintic, alexiteric, anodyne, constipating, urinary astringent, union promoter depurative, and tonic (Kalaiselvan, Gokulakrishnan, Anand, Akhilesh, & Velavan, 2013). Extract of this plant contains many secondary metabolites belonging to alkaloids, flavonoids, terpenoids, saponins, tannins carbohydrates, lignin, phenols, cardio glycosides, and sterols (Kalaiselvan et al., 2013; Soni et al., 2013).

A large number of polyphenolic compounds like ursolic acid, a-amyrenone, a-amyrin, b-amyrin, shoreaphenol, etc. are reported to be found in *Shorea robusta* bark (Soni et al., 2013). Such compounds contain aromatic rings for available π-electron and polyphenolic (–OH) groups for active sites and may be very effective for corrosion inhibition. Therefore, this study aims to study the corrosion inhibition efficiency of bark extract of this plant for mild steel corrosion in an acidic medium.

Research for greenery alternatives in the field of corrosion inhibition is forefront. Extract of various plant species has been used and reported as an inhibitor with very promising efficiency. There are some issues like ineffective at a higher temperature, about 90% inhibition by 100% inhibitor concentration, corrosion inhibition mechanism, etc. are to be addressed, for which further research should be conducted. These limitations can be minimized by selecting suitable phytochemicals. Phytochemicals vary from plant to plant, so, in this research phytochemicals from *Shorea robusta* will be studied.

CHAPTER – 3
MATERIALS AND METHODS

3.1 Collection and Pretreatment of Plant Material

Barks of *Shorea robusta* were collected from the forest of Bardiya District (Latitude: **28.27,** Longitude: **81.53**). The collected bark sample was washed with tap water properly to remove attached specks of dust and dried in shade. Dry bark was chopped into small pieces and kept it 9 days for shade dry then dried bark was grounded into a fine powder using a grinding machine.

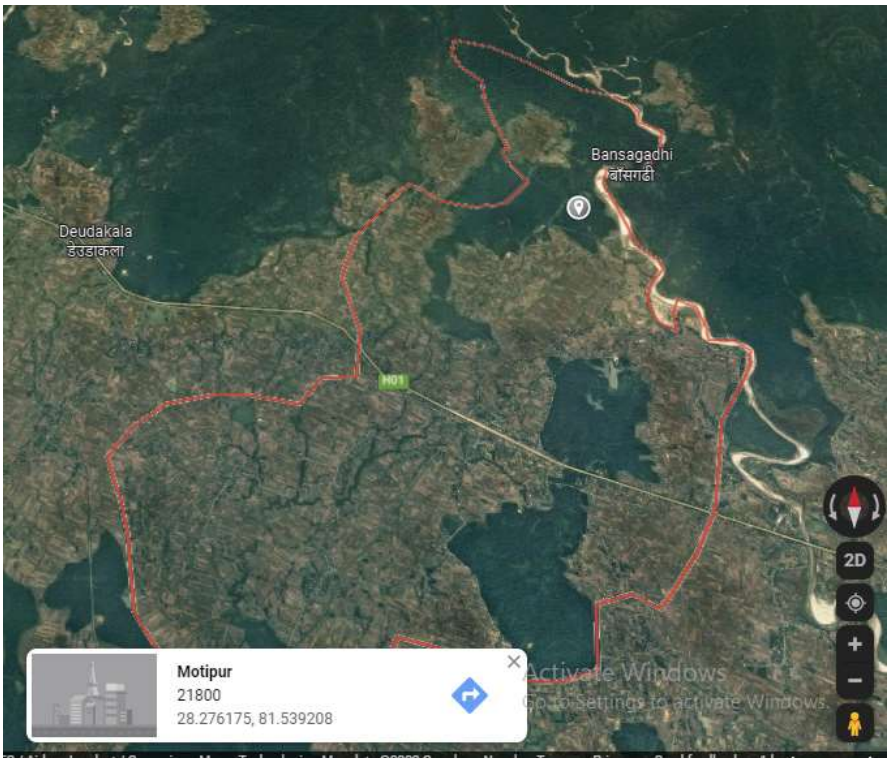

Figure 4: Google map of the sample collection area

3.2 Extract Preparation

The methanol extract was prepared by mixing 100 g of powdered sample and was soaked into 500 mL of hexane (Qualigens, sp. gravity: 0.660-0.675, purity %: 98.998%) in a glass vessel for 24 hours at room temperature. After one day the mixture was filtered. The filtrate contains nonpolar organic compounds that were not of our interest but are left for air dry for the measurement of UV as IR spectra. In the

residue, 500 mL methanol (Fischer scientific) was added and it was kept in an ultrasonicator for about 1.5hr. Ultrasonicator vibrates the compound at the molecular level and mixes the solvent and bark powder properly to extract chemical constituents (alkaloids, flavonoids, polyphenols, and various polar and semipolar organic compounds) present in it. The mixture was then filtered and the filtrate was taken as methanol extract (A).

3.3 Phytochemical tests of methanol extract (A)

For a phytochemical test, the required reagents were freshly prepared in the laboratory by the following process.

- **Preparation of Mayer's reagent**

Mayer's reagents were prepared by dissolving 1.3 g of mercuric chloride ($HgCl_2$) and 5 g of potassium iodide (KI) in 100 mL distilled water in a 100 mL volumetric flask.

- **Preparation of Dragondeorff's reagent**

Dragendorff's reagent was prepared by dissolving 3 g of Bismuth nitrate in 4 N of 8 mL sulphuric acid in one beaker and in another beaker dissolving 12 g Potassium iodide in 18 mL distilled water and mixing them to give an orange-red colored solution.

- **Preparation of 5 % $FeCl_3$ Solution/ Limbermann's reagent**

For the preparation of Limbermann's reagent, 5 g of Ferric chloride was dissolved in 100 mL of distilled water.

- **Preparation of Molish reagent**

For the preparation of molish reagent, alpha-naphthol was taken and its saturated solution was prepared by dissolving in ethanol.

- **Preparation of 5 % NaOH solution**

For the preparation of 5 % NaOH solution 5 g NaOH was weighted and dissolved in 100 mL distilled water.

3.4 Extraction/Isolation of Alkaloid

The filtrate methanol extract (A) was taken in a 1000 mL beaker and acidified using 5 % tartaric acid. During this process, 52.5 mL of tartaric acid was added to maintain pH≈3.5. In the acidified solution, alkaloids are assumed to get precipitated by forming salts with acid. The acidified solution was filtered, and the residue was made alkaline pH>10 by adding (46.5 mL) ammonia. In the alkaline medium, 1°, 2°, and 3°

alkaloids became free from salt. This solution was then kept in a separating funnel with the addition of an equal amount of dichloro methane (DCM) (Fischer scientific, 99 %, sp. gravity: 1.324) and shaken well to separate the aqueous and organic layers. The lower layer was the DCM layer and the upper layer is an aqueous layer. The organic layer was collected in a beaker as it contains alkaloids. The organic layer was made concentrate using a rotatory evaporator (IKA, RV 10) and then evaporated in a water bath using a thermostat (Clifton-45536) until it becomes semi-dry.

3.5 Extraction of Polyphenols

To separate the phenolic phase and non-phenolic phase, three drops of 6 N HCl were added to acidify the aqueous solution (filtrate from the previous experiment) and an equal amount of ethylacetate was added and the mixture was then kept in a separating funnel and shaken well to separate the aqueous and organic layers. The organic layer was collected in a beaker as it contains polyphenol. The organic layer was made concentrated by using a rotatory evaporator and then evaporated in a water bath until it becomes dry.

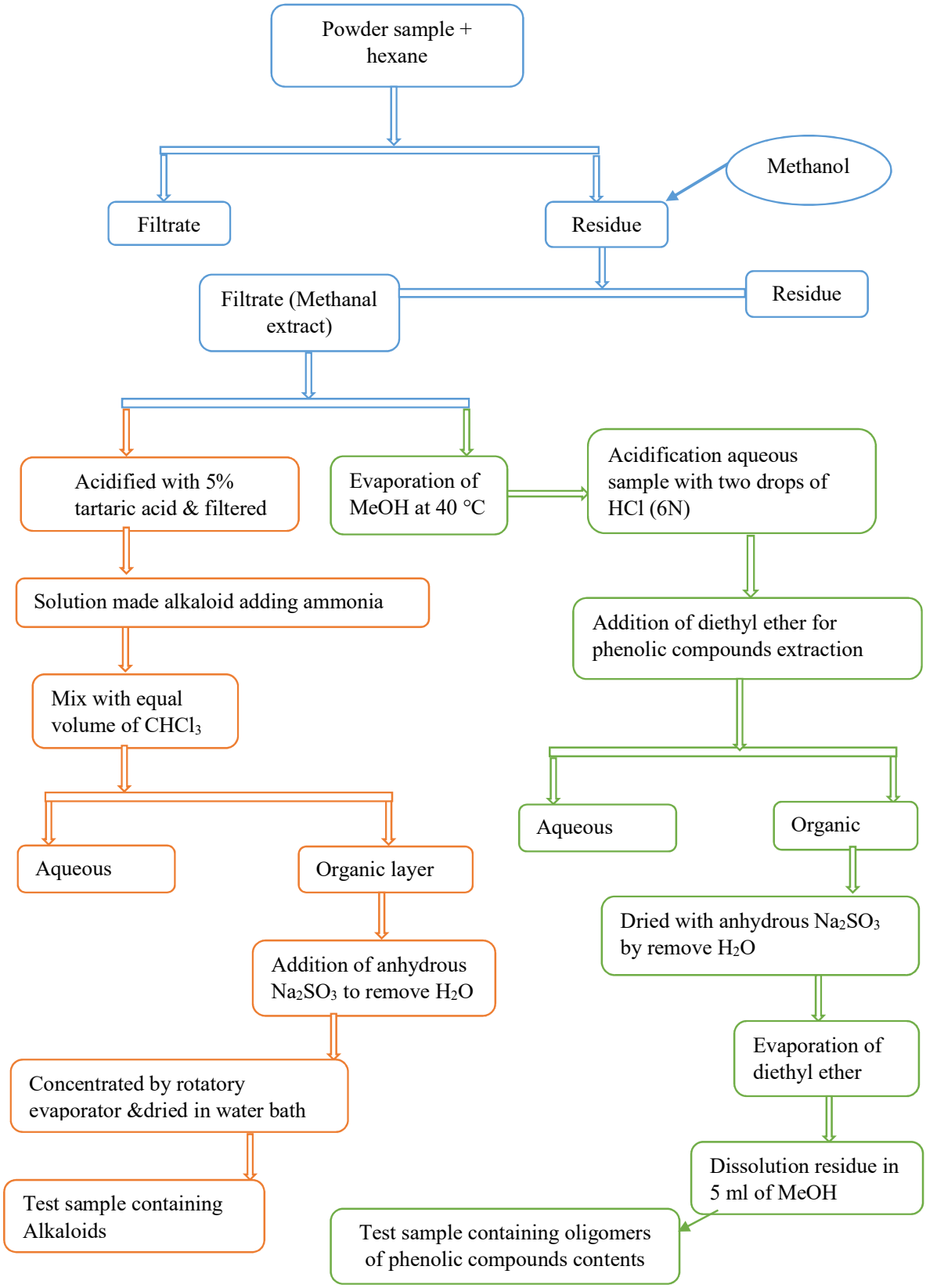

Figure 5: Flow chart diagram of extraction of alkaloid and polyphenol.

3.6 Preparation of corrosive Environment

For the preparation of the aggressive solution, concentrated H_2SO_4 (Fischer scientific, 97 %, sp. gr. 1.835 g/mL) was used. The required volume of concentrated acid was taken in a 1000 mL volumetric flask, containing distilled water, and diluted by adding distilled water up to mark.

3.7 Preparation of Inhibitor Solution

The inhibitor stock solution was prepared by dissolving 1 g of extract in 1000 mL of 1M H_2SO_4. The mixture was filtered to remove the undissolved part and the filtrate was transferred to a 1000 mL volumetric flask and 1 M H_2SO_4 was added up to mark. From the1000 ppm of stock solution, these concentrations (200, 400, 600, and 800 ppm) of inhibitor solutions were prepared by serial dilution.

3.8 Preparation of Mild Steel Sample

The mild steel (MS) coupons of dimension (4x4x0.2) cm^3 were taken from the local market of Thamel, Kathmandu. Before experimenting, Silicon Carbide (SiC) paper of different grades (400, 600, 800, 1000, and 1200) was used to polish the mild steel, washed with hexane to remove organic impurities followed by sonication in ethanol. Then dimension of each coupon was measured by a using digital vernal caliper before each experiment.

3.9 Test for Alkaloid

After extraction of alkaloid, the qualitative test was carried out using simple laboratory chemical methods such as Mayer's test and Dragendorff's test.

3.9.1. Mayer's test

In 2 mL DCM extract 3 drops of Mayer’s reagents were added and the appearance of a yellow precipitate indicates the presence of alkaloids.

3.9.2. Dragendorff's test

In 2 mL DCM extract on the addition of 3-4 drops of Dragendorff’s reagent was added, the appearance of orange-yellow ppt indicates the presence of alkaloid.

3.10 Test for Polyphenols

The presence of polyphenolic compounds in extracted solution was examined by a few drops of 5 % $FeCl_3$ were added to 2 mL acidified ethylacetate extract, the appearance of a black precipitate indicates the presence of polyphenols.

3.11 Inhibition monitoring

3.11.1 Weight Loss Measurement

The weight loss measurement was applied to examine the corrosion by immersing the MS coupons into the acid solution in the absence and presence of different concentrations of inhibitors. While monitoring corrosion rate, the dimension of MS coupons was measured, and immersed in inhibitor solution of different concentrations (0, 200, 400, 600, 800, 1000 ppm) at a different time.

The weight of MS was measured by using a 4-digit weight balance (Phoenix instrument-PH2204C) before and after immersion tests into aggressive and inhibitor solutions. The annual corrosion rate and inhibitor efficiency were calculated using equations 11 and 12 respectively.

$$Corrosion\ rate\ \ \upsilon = \frac{87600 \times \Delta W}{\rho \times A \times T} \qquad \ldots 11$$

$$(IE\%) = \frac{\Delta W_a - \Delta W_p}{\Delta W_a} \times 100 \qquad \ldots 12$$

Where,

ΔW = weight loss in gram

A = area in cm^2

ρ = density in g/cm^3

T= Time in hours

ΔW_a= Weight loss in absence of an inhibitor

ΔW_p= Weight loss in presence of an inhibitor

3.11.2 Electrochemical Measurement

In electrochemical measurement, the open circuit potential (OCP) and potentiodynamic polarization were carried out, and an electrochemical cell setup was arranged by taking MS coupon as a working electrode, graphite as a counter electrode, and a saturated calomel electrode as a reference electrode. The OCP measurement in different concentrations of inhibitor solutions was carried out for 30 minutes, before polarization measurement.

In potentiodynamic polarization, the sample was subjected to cathodic and anodic polarization, in the potential window -0.8 to 0 (V) i.e. ±300 mV from OCP in different concentrations of inhibitor for both immersed and as-immersed conditions.

3.12 FTIR Spectroscopic Analysis

FTIR spectroscopy is a powerful tool that can be used to identify the type of bonding, aromatic and aliphatic nature of compounds as well as functional groups present in the organic compounds. Since the extract contains organic compounds and these organic compounds are assumed to be adsorbed on the metal surface for protection against corrosion. So, FTIR characterization of phytochemical fraction, as well as MS surface adsorption, was carried out.

3.13 UV-Spectrophotometer Analysis

Ultraviolet-visible (UV-Vis) spectrophotometry is a technique used to measure light absorbance across the ultraviolet and visible ranges of the electromagnetic spectrum. When incident light strikes matter it can either be absorbed, reflected, or transmitted. The UV frequency is between 200 and 400 nm, and the visible spectrum is between 400 and 700 nm**.** It gives the spectra in the plot of absorbance (arbitrary units) vs wavelength (nm) where absorbance was measured by using Beer's Lambert's law as,

$$A = \varepsilon \times l \times C \qquad \ldots 13$$

Where,

A= Absorbance/Optical density

l = Path length of the sample

E= Molar absorptivity

C= Molar concentration.

CHAPTER – 4
RESULTS AND DISCUSSION

The characterization of extracted phytochemical was carried out by chemical tests, UV measurement, and FTIR spectroscopic measurements. The corrosion inhibitory behavior of the plant extract was studied by the weight-loss method, open circuit potential, and potentiodynamic polarization.

4.1 Qualitative tests of phytochemicals of *S. robusta*

Qualitative chemical test methods for the different phytochemicals in the methanol extract of *S. robusta* bark were performed in the laboratory are reported in table 1.

Figure 6: Phytochemical screening of methanol extract.

The phytochemical results the methanol extract of *S. robusta* contain less amount of alkaloid, Flavonoids, Glycosides, less amount of terpenoids, saponins, polyphenol, and less amount of quinine.

Table 1: Phytochemical screening of the Methanol extract solution.

S.N.	Experimental	Observation/Results	Interference
1.	**Test for Alkaloids**		
	Mayer's test 3 drops of Mayer's reagent + 2 mL extract, shaken well	Yellow ppt obtained	Presence of alkaloids
	Dragendorff's test 3 drops of Dragendorff's reagent + 2 mL extract, shaken well	Yellow ppt obtained	Presence of less amount of alkaloids
2.	**Test for Flavonoids** 5 mL dilute Ammonia solution + 3mL extract + conc. Sulphuric acid side of the test tube.	Yellow color appeared	Presence of alkaloids
3.	**Test for Glycosides** 3 drops Molisch's reagent + 2 mL extract, shaken well, and a few drops conc. Sulphuric acid was added side-wise and allow to stand for a few minutes.	Violet ring formed at the junction of two layers	Presence of glycosides
4.	**Test for Polyphenols** 3 drops of 5% $FeCl_3$ + 2 mL extract was shaken well.	Black color observed	Presence of polyphenols
5.	**Test for Terpenoids** In 2 mL $CHCl_3$ + 5 mL extract, 3 mL conc. H_2SO_4 was added side wise.	Less reddish-brown coloration observed	Presence of less amount of terpenoids
6.	**Test for Saponins** In 5 mL methanol extract, 20 mL distilled water was added and shaken vigorously.	Frothing appeared	Presence of saponins
7.	**Test for Quinones** In 2 mL methanol extract conc. HCl was added.	Yellow-colored ppt was obtained	Presence of quinones
8.	**Test for Proteins** In 2 mL methanol extract, 2 mL of 5% NaOH and 3 mL of $CuSO_4$ were added.	Before the addition of $CuSO_4$ brown ppt obtained	Absence of Protein

4.2 FTIR Analysis

The spectrum of FTIR provides information about the molecular structure and conformation of organic molecules as well as different functional groups present in the sample. It is useful to identify the carbon-heteroatom bond from their stretching frequency in the FTIR spectrum.

FTIR spectrum of hexane fraction, DCM fraction (Alkaloid), Ethylacetate fraction (Polyphenols), and methanol extract of *S. Robusta* was recorded by PerkinElmer Spectrum (IR Version 10.6.2) FTIR spectrometer present in Department of chemistry Amrit Campus.

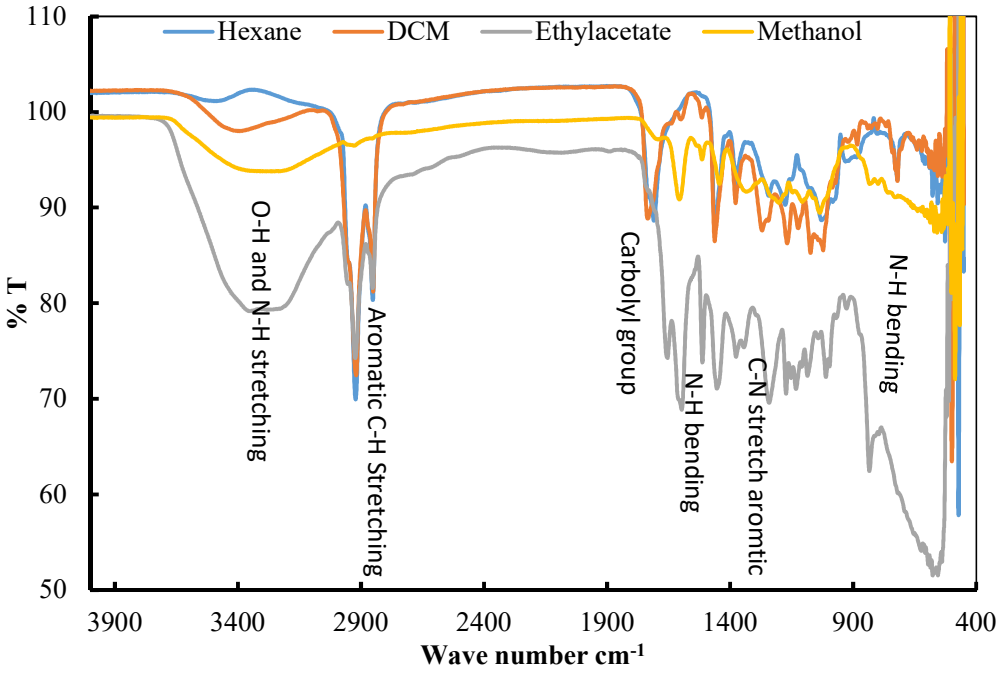

Figure 7: IR- spectrum of S. Robusta bark in different kinds of extracts.

The broad absorption peak at 3200-3400 cm^{-1} is due to O-H stretching and N-H stretching of secondary amine. The sharp peak at 2922 cm^{-1} is due to the aromatic C-H stretching of alkane and the splitting peak at 2851 cm^{-1} is due to the C-H stretching of the aldehyde group. The splitting peak at 1697 cm^{-1} is due to C=O stretching of the amide group and the peak at 1598 cm^{-1} is N-H bending of amine. The medium peak at 1357.88 cm−1 is due to the bending vibration of O-H bending of 26 alcohol. Similarly, the absorption peak at 1454 cm^{-1} is due to the C-N stretching of aromatic

amine, absorption at 836 cm $^{-1}$ N-H bending was for only primary and secondary amines (Silverstein & Bassler, 1962; Sundararajan & Kumari, 2017).

4.3 UV-Spectrophotometer Analysis

The UV measurement is carried out for the identification of unsaturation or the presence of lone pair of electrons in the organic compounds. The UV spectra of non-polar hexane faction, Nitro group containing hetero compounds (Alkaloid), Phenolic group containing Polyphenols, and direct methanol extract have been recorded using Labtronics, LT-2802 double beam ultraviolet-visible (UV-Vis) spectrometer in Amrit Campus, Kathmandu.

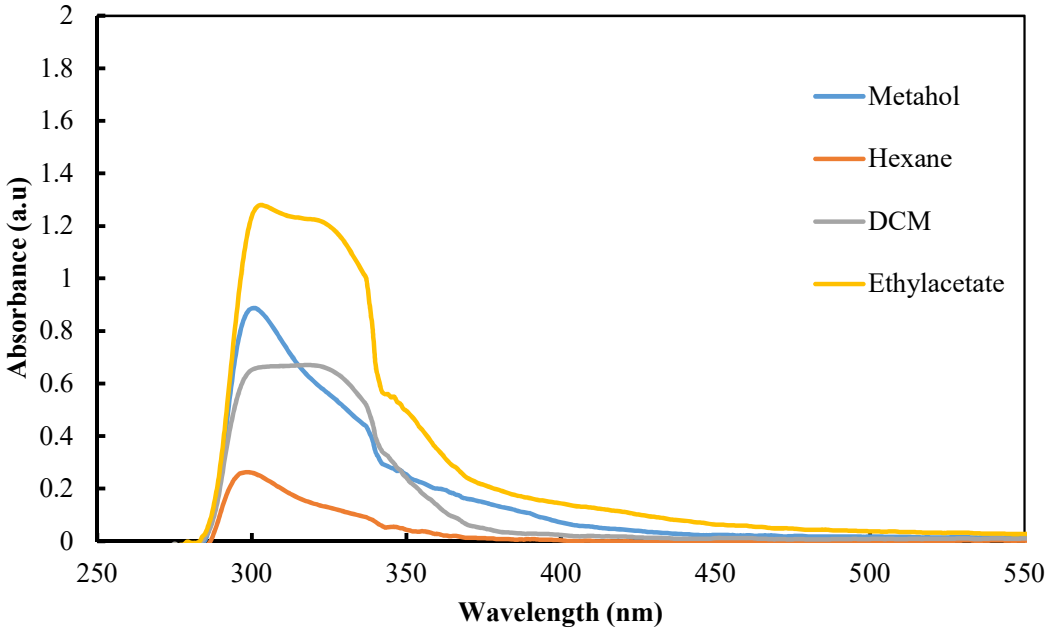

Figure 8: UV-Visible spectrum of S. Robusta bark in different kinds of extracts.

The absorption of electromagnetic radiation was divided into near ultraviolet when absorption takes place at (200 nm to 380 nm). And it is mostly due to π-π*. The UV/Vis spectra of polyphenols are generally attributed to electronic transitions between p-type molecular orbitals (MOs), which are more or less extended over the molecular backbone, depending on the subclass as defined above.

In the given spectra, the sharp peak was found at 303 nm and 324 nm with an absorbance of 1.28 and 1.208 respectively in the extract of ethyl acetate. Which indicates the presence of polyphenolic compounds gives the π-π* transition due to unsaturation (Gierschner, Duroux, & Trouillas, 2012). The given spectra of the

methanol extract were found to be 301nm with an absorption of 0.887 a. u. This is also due to π-π* transition of organic compounds.

Similarly, the absorption peaks of the DCM fraction give the broad peak at 311-327 nm with an absorbance of 0.67 a. u. and the hexane fraction also gives the maximum absorbance at 299 nm with an absorbance of 0.263 a. u. indicates the presence of unsaturated organic compounds having π-π* transition (Mohammed, 2018; Silverstein & Bassler, 1962).

4.4 OM Image of Sample

An optical microscopic (OM) image of the policed MS as well MS coupons immersed in the acid and 1000 ppm green inhibitor for 1h was taken by using an light plarizing microscope, Radical Scientific, India, in the Laboratory of Professor Dr. Amar Prasad Yadav, Central Department of Chemistry T. U. in different resolutions (4x, 10x, 40x). The optical image of MS surfaces that are dipped in acid and the presence of green inhibitors in different magnifications are shown in the following figure 9. The formation of corrosion products (small pits and rusts) is observed in acid than in presence of inhibitor, while no corrosion products seem in policed (undipped) MS co upons.

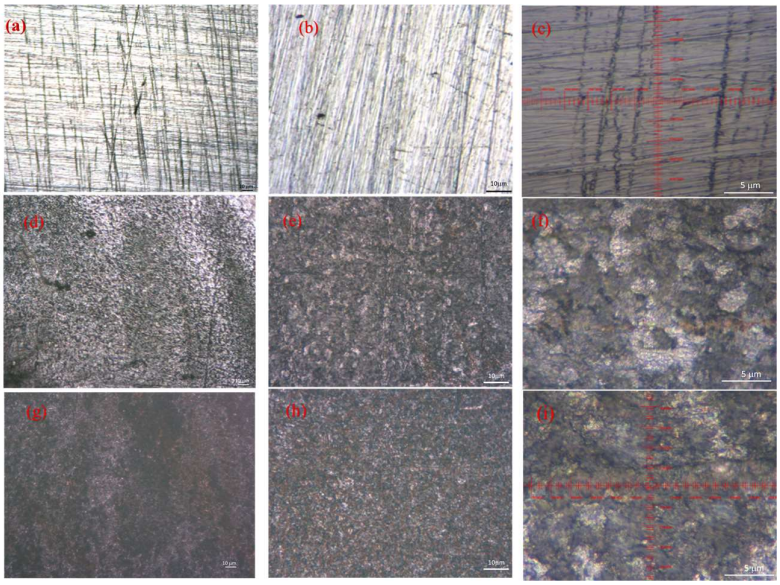

Figure 9: OM Image of Polished MS coupons (a). At 4X (b). 10X (c). 40X magnification; MS coupons dipped in acid (d). At 4X (e). 10X and (f). 40X magnification ; and MS coupons dipped in 1000 ppm inhibitor (g). At 4X (h). 10X and (i). 40X magnification.

4.5 Weight loss measurement of *S. robusta*

The alkaloid contain in the bark of *S. robusta* was very less amount so it was not isolated in measurable quantity. In the weight loss measurement, methanol extract and polyphenols were used as an inhibitor.

When MS coupons are dipped in the aggressive solution, the interaction with the aggressive environment takes place resulting in the formation of corrosion products. After the formation of the corrosion product, the weight of MS gets decreased. The decrease in the weight of MS coupons is related to the nature of the MS surface, temperature, and concentration of the inhibitor solutions.

4.5.1 Weight loss of MS in different concentrations of polyphenols.

The weight loss measurement data obtained using polyphenols as an inhibitor are represented in table 2. The results obtained are far away from theoretical assumptions. This may be due to the synergetic effect of OH- ions with acid to increase corrosion rate. It seems that polyphenol supported the acid for further increase in corrsion rate. It is also represented in figure 10.

Table 2: Variation of weight loss (g/cm^2) with different immersion time at different concentrations of Polyphenol as an inhibitor.

Time (h)	Weight loss (g/cm^2)					
	Acid	200ppm	400ppm	600ppm	800ppm	1000ppm
0.5	0.001144	0.001608	0.001838	0.001458	0.001442	0.001076
1	0.0077	0.01147	0.00911	0.0128	0.0054	0.0099
3	0.00199	0.004038	0.00383	0.00347	0.00288	0.00225

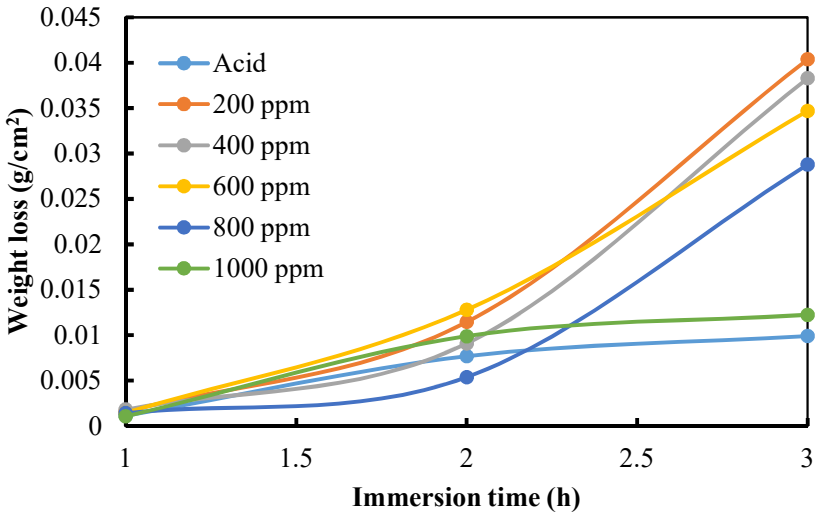

Figure 10: Variation of weight loss of MS in different concentrations of polyphenol at temperature 20 ℃.

4.5.2 Effect of Immersion time on weight loss of MS

When the methanol extract solution was added to the aggressive environment then it reduces the weight loss. The loss in weight of MS was very high in absence of an inhibitor and it gradually decreased with an increase in inhibitor concentration. The weight loss of MS in the presence and absence of an inhibitor was carried out at different immersion times in 1M H_2SO_4. The result of the weight loss measurement shows that the presence of methanol extract as an inhibitor reduced the weight loss of MS in the acidic medium as compared to that of 1M sulfuric acid. The experiments were performed in different time intervals i.e. 1/2, 1, 3, 6, and 24 hours. The observed weight loss data at different immersion times are tabulated in table 3 and figure 11.

Table 3: Variation of weight loss (g/cm^2) with different immersion time at different concentrations of Methanol as an inhibitor.

Time (h)	Weight loss (g/cm^2)					
	Acid	200ppm	400ppm	600ppm	800ppm	1000ppm
0.5	0.000567047	0.000638123	0.000556525	0.000233957	0.000221826	0.000161732
1	0.00315469	0.001966064	0.002183493	0.001977888	0.001302675	0.001043967
3	0.0090257	0.007208564	0.005712579	0.003885291	0.004946844	0.004262203
6	0.013235741	0.014389067	0.01249425	0.009720692	0.008372671	0.007534578
24	0.050522374	0.047224023	0.027122728	0.036765858	0.035148724	0.023310907

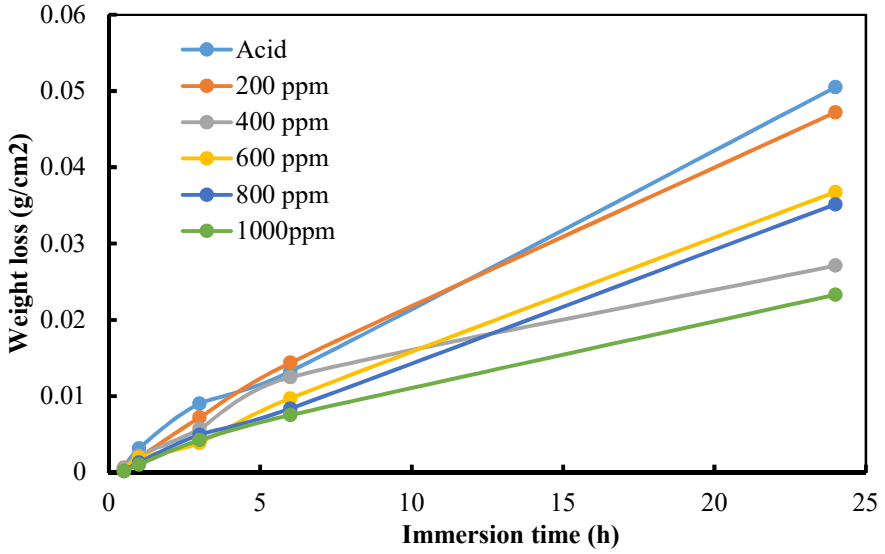

Figure 11: Weight loss of MS in different concentrations of inhibitor at temperature 18 ℃.

It is found that with the concentration of the inhibitor the weight loss of MS coupons decreases significantly. It may be due to the adsorption of inhibitor molecules on the MS surface and form the diffusion barrier to electrochemical corrosion reaction.

4.5.3 Variation of corrosion inhibition efficiency with Inhibitor Concentration

From the study of weight loss measurement, it was found that the inhibition efficiency for mild steel was higher at a higher concentration of inhibitor (methanol extract). The experiment was carried out in the different concentrations (0, 200, 400, 600, 800, 1000 ppm) of inhibitors in 1M H_2SO_4. The weight loss data indicates that the inhibition efficiency increases as the increase in concentration. It is because, at higher concentrations, a large number of molecules are available for adsorption onto the MS surface. The maximum inhibition efficiency is found to be 71.47% at ½ hours immersion time in 1000 ppm inhibitor concentration. This efficiency didn't remain constant on increasing immersion time. The minimum efficiency of 1000 ppm inhibitor concentration was found to be 43.1% at 6 hours. The observed variation of efficiency with concentration (600, 800, and 1000 ppm) at room temperature 18 °C was measured by using weight loss measurements was shown in table 4 & figure 12.

Table 4: Variation Efficiency with different immersion time at different concentrations of Methanol extract as an inhibitor.

Time (h)	Efficiency %		
	600ppm	800ppm	1000ppm
0.5	58.74115099	60.88054699	71.47823134
1	37.30323064	58.70670587	66.90747224
3	56.9530169	56.38458198	66.47244615
6	26.55725218	36.74195903	43.07400281
24	27.2285612	30.42938873	53.86023068

The obtained value tabulated in table 4 reveals that the inhibition efficiency of the inhibitor below 6 h immersion is good however there is highly decline in the efficiency. This indicates that the equilibrium between adsorption and desorption of inhibitors in the MS surface took a very large time. This also implies that there is physical adsorption between the inhibitor and MS surface.

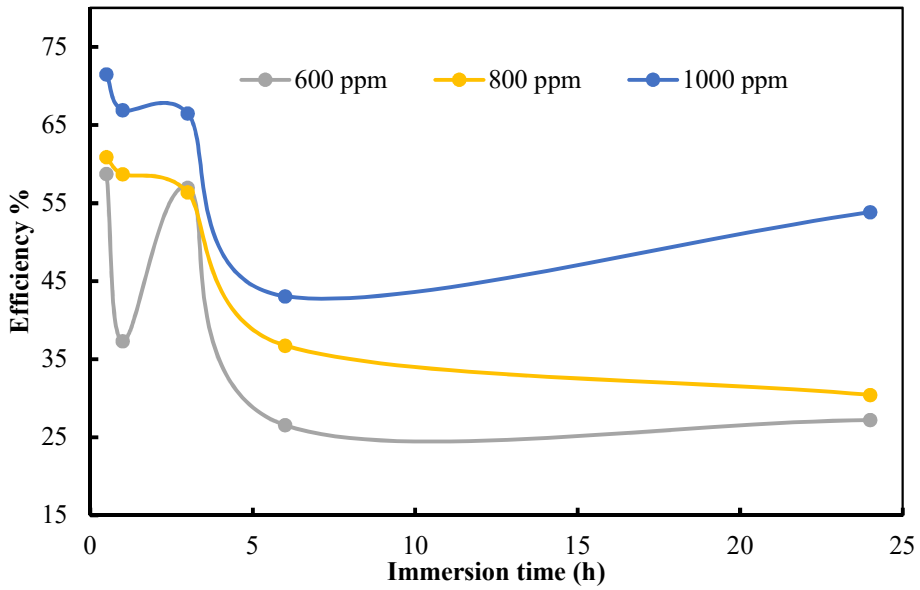

Figure 12: Variation of inhibition efficiency vs time of the corrosion of MS in 1M H_2SO_4 solution at various times of immersion.

4.5.4 Variation corrosion rate with immersion time.

The variation of corrosion rate with immersion time was studied in 1M acid in the presence and absence of an inhibitor. The rate of corrosion of MS is very high in

absence of an inhibitor and it gradually decreased with an increase in the concentration of inhibitor.

Table 5: Variation of corrosion rate with different immersion time at different concentrations of Methanol extract as an inhibitor.

Time (h)	Corrosion Rate (mm/yr)					
	Acid	200ppm	400ppm	600ppm	800ppm	1000ppm
0.5	0.126395165	0.14223819	0.12404994	0.05214919	0.049445097	0.036050137
1	0.351591358	0.219118572	0.243351087	0.220436423	0.145183654	0.116350468
3	0.335305889	0.267799068	0.212223028	0.144339069	0.146245065	0.112419862
6	0.245854737	0.26727784	0.232081495	0.180562474	0.15552289	0.139955261
24	0.234614078	0.219297306	0.125951598	0.17073204	0.163222448	0.108250394

The corrosion rate (mm/yr) of MS in different concentrations of inhibitor was calculated and shown in table 5. The variation of corrosion rate with immersion time was plotted in the graph below, which indicates that the rate of corrosion was high in acid and 200 ppm then decreases significantly with the increase in the concentration of inhibitor. The rate of corrosion is very low at 1000 ppm in all intervals of times

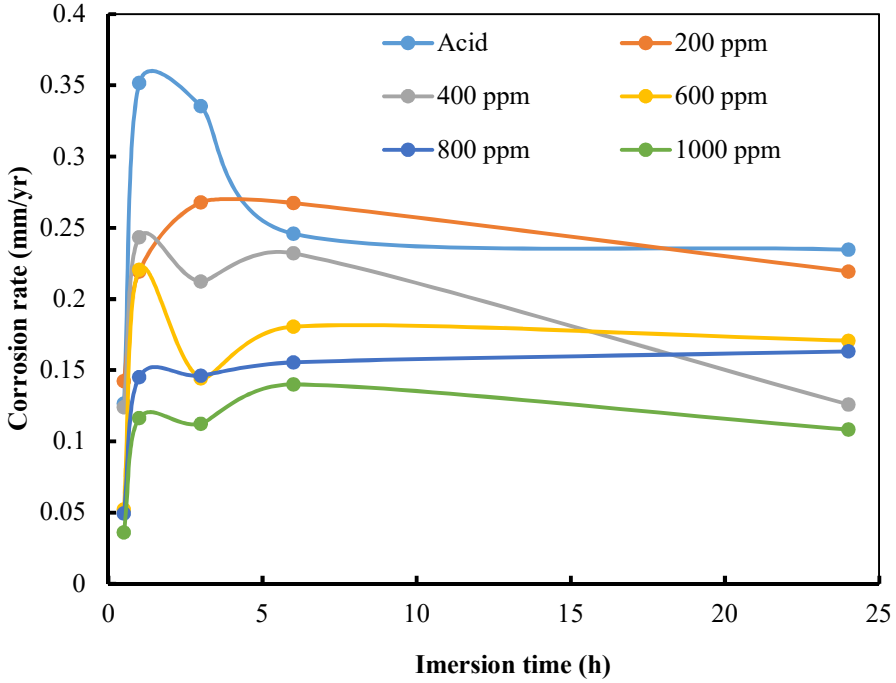

Figure 13: The variation of corrosion rate with immersion time at 18 ℃.

4.5.5 Weight loss with the different concentrations of Methanol Extract.

As MS coupons were dipped in the acid solution, the weight of coupons loosed due to the formation of corrosion products, and the weight of MS decreased. The loss of weight of mild steel in different concentrations of inhibitors was shown in the figure below.

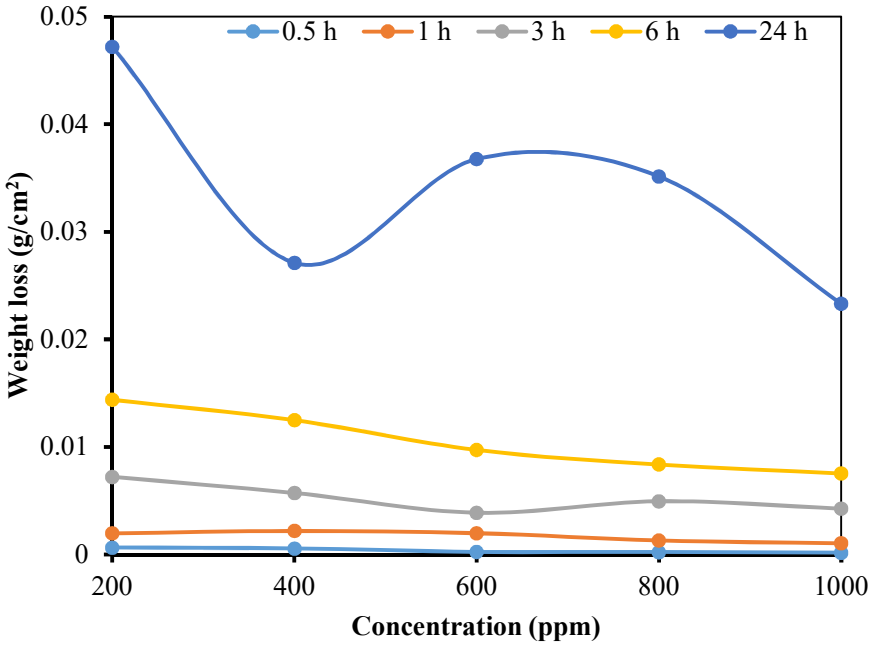

Figure 14: Variation of weight loss versus concentration of extract on mild steel in 1 M H_2SO_4 solution at various times.

4.5.6 Variation of weight loss with temperature in methanol extract.

The effect of temperature on the inhibition process was studied using the inhibitor solution of different concentrations (200, 400, 600, 800 & 1000 ppm). The weight loss measurement in these different inhibitor solutions in different temperatures was measured by taking reference to the acid solution. For this measurement, the MS coupons were immersed in these solutions for one hour at different temperatures (18, 28, 38, 48, 45 & 58 °C). Observed data are tabulated in table 6.

Table 6: Variation Weight loss with different temperature at different concentrations of Methanol extract as inhibitor.

Temperature (^{0}C)	Weight loss (g/cm^2)					
	Acid	200ppm	400ppm	600ppm	800ppm	1000ppm
18	0.0031546	0.00196606	0.00218349	0.00197788	0.00130267	0.00160323
28	0.00716745	0.00371082	0.00377312	0.00412336	0.00319611	0.00248775
38	0.01056349	0.00927586	0.00673871	0.00555190	0.00467223	0.00427071
48	0.01839668	0.01611672	0.01273772	0.0110893	0.00987327	0.00926548
58	0.02470672	0.02227481	0.01807069	0.01697193	0.01548455	0.01549319

.

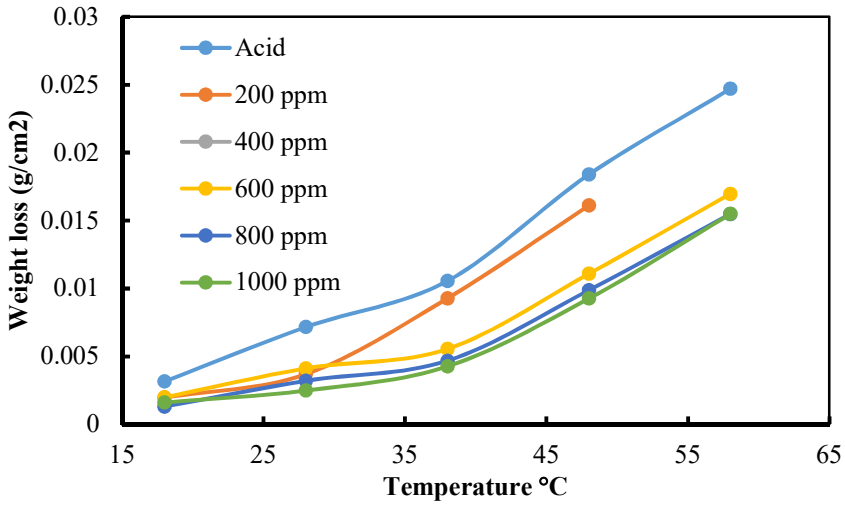

Figure 15 ; Variation of weight loss of MS with temperature in the presence and absence of inhibitor.

The variation of weight of MS in different concentrations of inhibitor with temperature is shown in figure 14. In the graph it is clear that the weight of MS was increased gradually with increasing temperature, it is because the hydrogen evolution reaction takes place so rapidly at increasing activation energy with higher temperature.

4.5.7 Inhibition efficiency with temperature by different concentrations of methanol at a different time of immersion.

The efficiency of the inhibitor was also varied with the temperature. The effect of temperature on the corrosion inhibition with and without inhibitors was studied with

different temperatures at a constant immersion time. Thus obtained data are tabulated in table 7. As in the table, it is clear that the inhibition efficiency is maximum at 28 °C. Above the 28 °C the inhibition efficiency at 200 ppm is almost negligible but at higher concentrations, it showed somewhat inhibition. Whenever it has lower efficiency at normal temperature, it is stable up to higher temperatures also. It was very interesting that the methanol extract of *S. Robusta* was not decomposed even at 50 °C temperature. So it can be claimed that the 1000 ppm methanol extract prepared from *S. Robusta* can work at higher temperatures up to 48-50 °C.

After these results, it can be concluded that the structural deformation of molecules may occur more than that of the desorption of molecules from the MS surface. This deformation leads to the decrease in inhibition efficiency of inhibitors for MS in the acidic medium above 58 °C.

Table 7: Inhibition efficiency (%) of the inhibitor of different concentrations on MS at different temperatures.

Temperature (°C)	Efficiency %				
	200ppm	400ppm	600ppm	800ppm	1000ppm
18	37.67805511	30.7858166	37.30323064	58.70670587	49.17933237
28	48.2268118	47.3574879	42.4710547	55.40798317	65.29094784
38	12.18941727	36.20753385	47.44251575	55.76993539	59.57098745
48	12.39332162	30.76075426	39.72088014	46.33121242	49.63505221
58	9.843115844	26.85920067	31.3064102	37.32657241	37.29161409

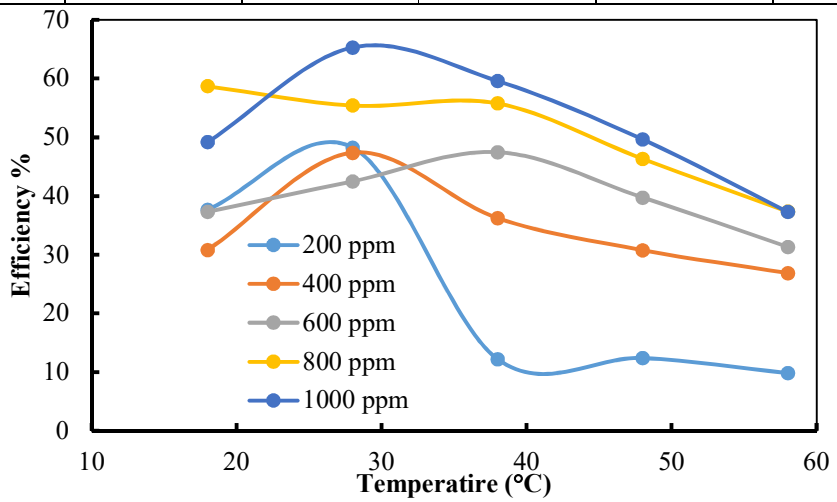

Figure 16: Variation of Inhibition efficiency with temperature by different concentrations of methanol extract in 1M H_2SO_4.

The inhibition efficiency dependence on temperature was studied and shown in the figure below. The maximum efficiency of 65.3% at 1000 ppm inhibitor at 28 ℃ temperature was achieved. The loss in weight of MS was very high in absence of an inhibitor. Besides inhibitors, the loss in weight of MS gradually decreases with an increase in the concentration of inhibitors as shown in Figure 16. It may be due to the adsorption of inhibitor molecules on the metal surface. The minimum weight loss was observed in the 1000 ppm solution at 0.5 hours of immersion.

4.6 Adsorption Isotherm

MS coupons are immersed in the acid and the inhibitor solution. When MS is immersed only in the acid solution the acid molecules get adsorbed on the metal surface and a vigorous reaction occurs causing deterioration of MS coupon. When MS coupons were immersed in the inhibitor solution, acid, as well as bulky organic molecules of inhibitors, were also adsorbed on the MS surface. These molecules blockage the active sites (anodic and cathodic) and the reaction between the metal surface and acid molecule was restricted (Ijuo, Chahul, & Eneji, 2016; Shukla & Ebenso, 2011).

For a clear explanation of this adsorption process, it is better to know the adsorption isotherm. For a better understanding of the adsorption isotherm and the type of adsorption between MS surface and inhibitor molecule, it is better to check adsorption isotherms. Adsorption isotherm gives the basic information on the interaction between the inhibitor and MS surface. It was assumed that at first water molecules adsorbed on the MS surface in an aqueous solution and accelerate the corrosion rate by reacting with metal atoms and oxygen molecules. After that in presence of an inhibitor, these adsorbed molecules are then replaced by inhibitor molecules. So, the adsorption of inhibitor molecules from an aqueous solution is a quasi- substitution process. To identify the adsorption isotherm, Langmuir, Freundlich, and Tempkin adsorption isotherms were determined (Andoor, Okeoma, & Mbamara, 2021; Ijuo et al., 2016).

4.6.1 Langmuir adsorption isotherm

Langmuir adsorption isotherm equation, the equation can be applied to find whether the adsorption process is monolayer or multilayer as,

$$\frac{C_{in}}{\theta} = \frac{1}{K_{ads}} + C_{inh} \qquad \dots 14$$

This equation is like the equation of a straight line as y = mx + c. The linear relation between the fraction of covered surface (θ) value and C_{inh} should be known to find the adsorption isotherm. The linear relation between the fraction of covered surface (θ) and molar concentration (C_{inh}) should be known to find the adsorption isotherm. Though this may not be enough and the mixture of alkaloids may not follow this trend. For the reference Gamma- Gurjunenepoxide molecule is taken to calculate the molar concentration of the inhibitor solution (Sushma, Pal, & Viney, 2017). If the slope of the curve obtained by plotting vs C_{inh} in the above equation is unity then it indicates the monolayer adsorption. As in the equation if one uses the molar concentration of the inhibitor then the value of adsorption constant K_{ads} can be calculated from the intercept of a straight line.

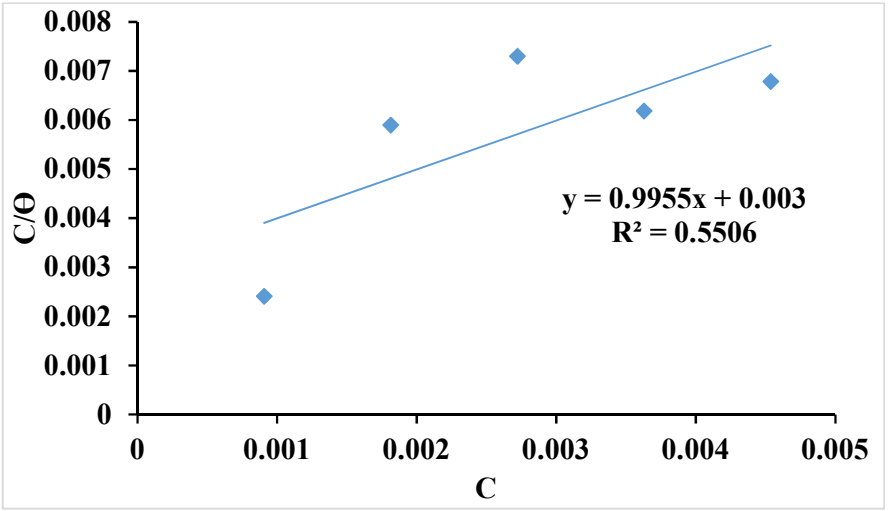

Figure 17: Langmuir adsorption isotherm plot for MS in 1 M H_2SO_4 with different concentrations of inhibitor.

From the above plot, it is found that the R^2 value of a straight line obtained by plotting $\frac{C_{inh}}{\theta}$ vs C_{inh} is 0.5506. This value highly deviates from the unity, which indicates the inhibitor molecules adsorbed on the MS surface did not obey Langmuir adsorption isotherm. This indicates that adsorption may be mono- or multilayer but the complete monolayer has not been formed before multilayer formation. Hence it can be concluded that this corrosion inhibition process cannot be explained by this Langmuir isotherm (Ituen, Akaranta, & James, 2017a).

4.6.2 Freundlich adsorption isotherm

Freundlich adsorption isotherm is the measurement of variation in the quantity of gas adsorbed by a unit mass of solid adsorbent of a system for a given temperature. It can be studied to know how easily the adsorption of inhibitor molecules on the MS surface. The Freundlich adsorption isotherm can be determined by using the following formula,

$$ln\theta = \frac{1}{n} lnC + lnK \qquad \ldots 15$$

This equation (15) is in the form of the equation of a straight line and when we plot $ln\theta$ vs lnC the R^2 value of the straight line is found to be 0.5379 with a slope of 0.3816.

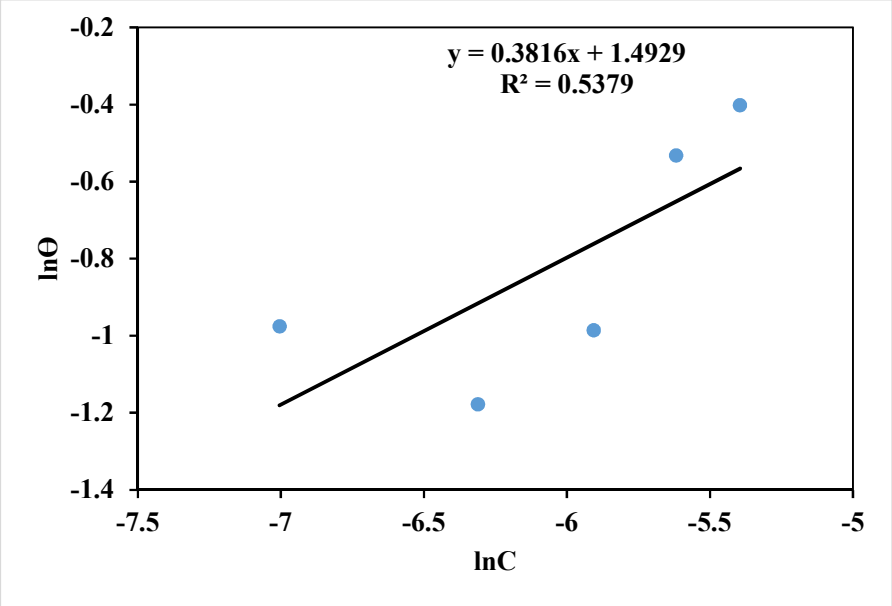

Figure 18 : Freundlich adsorption isotherm plot for MS in 1 M H_2SO_4 solution.

4.6.3 Temkin adsorption isotherms

The Temkin adsorption isotherm model assumes that the adsorption heat of all molecules decreases linearly with the increase in coverage of the adsorbent surface and that adsorption is characterized by a uniform distribution of binding energies, up to maximum binding energy. For the explanation of the corrosion inhibition mechanism and the nature of interaction taking place in the adsorbed layer Temkin adsorption isotherm, a plot of Θ against ln C has been plotted in the graph by using the following equation,

$$\theta = -\frac{1}{2a} lnC - \frac{1}{2a} lnK \qquad \ldots 16$$

The given plot shows that the R^2 value of adsorption of inhibitor in MS coupons is 0.5657 with molecular interaction parameter (a) -2.707 and 1.344 K value. We know that the value describes how strongly the inhibitor molecules are adsorbed on the metal surface (Ituen, Akaranta, & James, 2017b; Piccin, Dotto, & Pinto, 2011). Hence we conclude that the inhibitor molecules are not strongly absorbed on the MS surface.

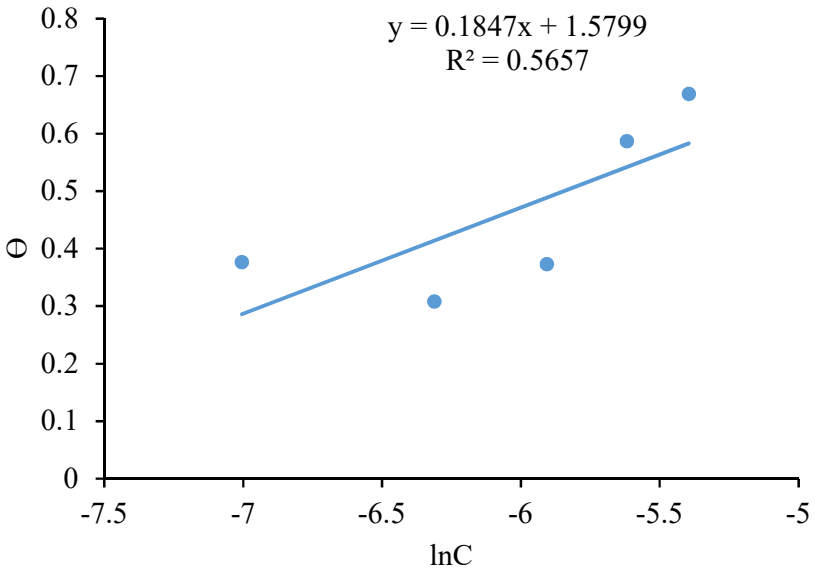

Figure 19: Temkin adsorption isotherm plot for MS in 1 M H_2SO_4 with different concentrations of inhibitor.

The slope and intercept values have their typical meanings as previously stated. The R^2 number represents the correlation between the measured values and hence helps in determining whether the measured values are acceptable. Table 7 shows three different R^2 values for three different isotherms. The R^2 value highly deviated from unity in the case of all three isotherms, indicating unusual adsorption of inhibitor molecule on MS surface and the inhibitor prepared by methanol extract of *S. robusta* doesn't follow any adsorption isotherm.

Table 8 : Different parameters obtained from three different adsorption isotherms.

Isotherm	Plotting	Slope	Intercept	R^2
Langmuir	C/Θ vs C	0.9955	0.003	0.5506
Freundlich	$ln\Theta$ vs lnK	0.3816	1.493	0.5379
Temkin	Θ vs lnK	0.1847	2.5799	0.5657

4.7 Activation Energy

Corrosion is an electrochemical reaction that takes place reaction between the metal surface and corrosive environment. The rate of corrosion reaction varies with temperature because the energy of activation increases with temperature. The activation energy of the reaction in the presence and absence of an inhibitor in a corrosion cell can be explained by rearranging the Arrhenius equation. The rearranged Arrhenius equation related to corrosion reaction is given as,

$$log(CR) = log\, A - \frac{E_a}{2.303RT} \quad \ldots 17$$

Where, T = Absolute temperature

A = Arrhenius pre-exponential constant E_a = Energy of activation

When we plot the graph between logarithms of the rate of corrosion to $\frac{1}{2.303RT}$ we obtain the value of activation energy from the slope of the straight line (Ijuo et al., 2016; Karki et al., 2021).

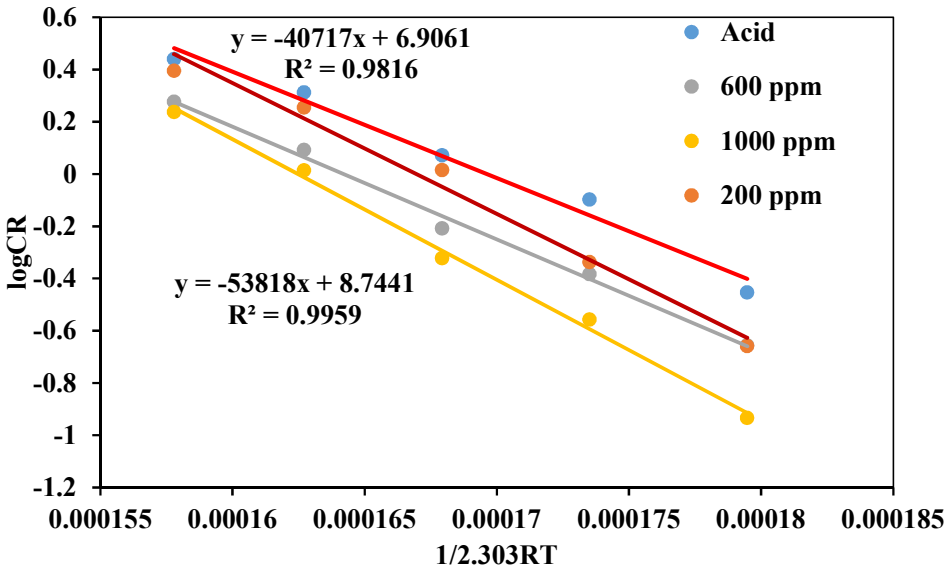

Figure 20: Arrhenius plot for MS in 1M H_2SO_4 with and without inhibitor.

The graph of the Arrhenius plot shows that the energy of activation of the reaction between MS surface and acid molecules is found to be 40.72 KJ/mol. In the addition of inhibitor, we found that the energy of activation of corrosion reaction increased to 50.04, 43.20, and 53.82 KJ/mol for 200, 600, and 1000 ppm inhibitors respectively. This increase in activation energy reveals that with the addition of an inhibitor,

inhibitor molecules suppress the reaction rate between acid and MS resulting in a decrease in corrosion rate. This increase of activation energy is < 20 KJ/mol hence we can say that the inhibitor molecules of methanol extract of *S. robusta* are adsorbed on mild steel samples from only the physisorption process.

4.8 Enthalpy and Entropy measurement

The enthalpy and entropy of the system can be calculated by using the transition state equation as,

$$\log(\frac{CR}{T}) = \log\left(\frac{R}{hN_a}\right) + \frac{\Delta S^o}{2.303R} - \frac{\Delta H^o}{2.303RT}$$

Where,

h = Plank's constant

N_a = Avogadro's number

ΔS^o = Entropy of activation

ΔH^o = Enthalpy of activation

When we plot the graph between $\log(\frac{CR}{T})$ vs $\frac{1}{2.303RT}$ we can determine the value of ΔH^o from slope the of straight line and value of ΔS^o from y-intercept of a line (Karki et al., 2021; Shukla & Ebenso, 2011).

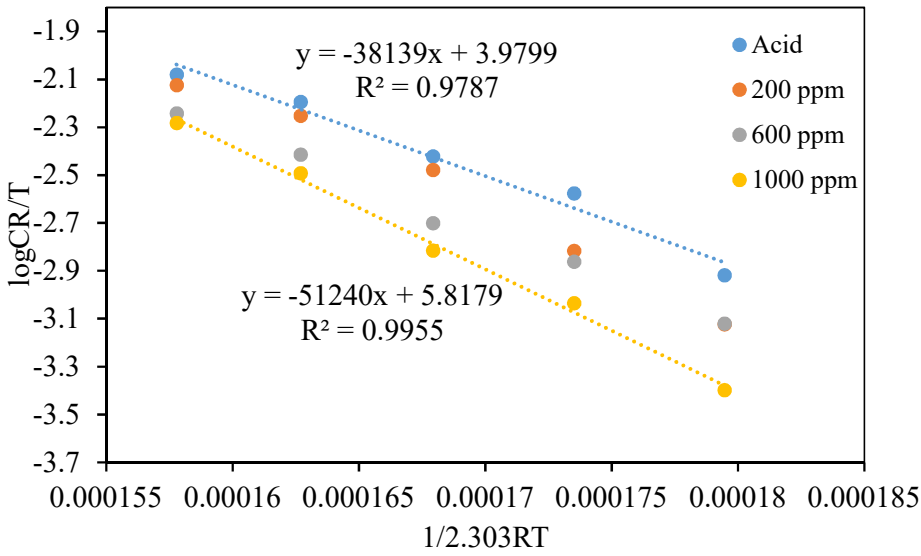

Figure 21: Transition state plot for MS in 1M H_2SO_4 with and without inhibitor.

From the transition state plot (figure 21) the enthalpy of the system in the absence of an inhibitor was found to be 38.14 KJ/mol and in presence of an inhibitor, it was observed that 47.47, 40.62 & 51.24 kJ/mol for 200, 600 and 1000 ppm inhibitor respectively. When we consider a 1000 ppm inhibitor the enthalpy of the system

increased by 13.1 kJ/mol. This increase in enthalpy indicates a decrease in the corrosion rate. The entropy of this system has been calculated from the intercept of the transition state plot. We found the entropy of activation is -121.411, -93.835, -117.773, and -86.175 J/K/mol for acid, 200, 600, and 1000 ppm inhibitor solution respectively.

These values of E_a, $\Delta H°$ and $\Delta S°$ supports the adsorption behavior of the inhibitor on the metal surface. The calculated values of all these thermodynamic parameters in the presence and absence of inhibitor are tabulated in the following table 9. The presence of an inhibitor increases the activation energy and reduces the reaction rate. In addition, this increase in activation energy indicates the adsorption of inhibitor molecules on the MS surface or coverage of the metal surface by forming a barrier (Ituen et al., 2017b; Karki, Choudhary, & Yadav, 2018).

Table 9: Activation parameters of the MS dissolution in 1 M H_2SO_4 without and with inhibitor.

Corrosive environment	**E_a (kJ/mol)**	**$\Delta H°$ (kJ/mol)**	**$\Delta S°$ (J/mol/K)**
1M Sulfuric Acid	40.72	38.14	-121.411
200 ppm inhibitor	50.04	47.47	-93.835
600 ppm inhibitor	43.02	40.62	-117.773
1000 ppm inhibitor	53.82	51.24	-86.175

4.9 Electrochemical measurements

4.9.1. Variation of open circuit potential (OCP) measurement

Open circuit potential (OCP) measurement is one of the simplest concepts and it is a method of the indirect corrosion monitoring technique. Mostly it was adopted for monitoring the corrosion rate of reinforcing steel in concrete and structures such as buried pipelines in soils under cathodic protection in the industry. OCP is the electrode potential at which no net current flow through the external circuit of the electrochemical cell. OCP of the corroding metal/alloy is measured in 3 electrodes system by using a potentiostat as a voltage between the working electrode (metal itself) and the reference electrode (SCE). The variation of OCP with time can be measured by determining the voltage difference between an MS immersed in a sample

solution and as an appropriate reference electrode along with the counter electrode (Bhattarai, 2008).

The variation of open circuit potential (OCP) of mild steel in 1M H_2SO_4 was studied by monitoring changes in corrosion potential (ϕ_{corr}) with time. The OCP changes of mild steel were measured for 30 min at room temperatures immersed and without immersed in acid and inhibitor solution at different concentrations (200, 400, 600, 800, and 1000 ppm). The measured OCP to time by using potentiostat ((Hokuto-Denko, HA-151) Laboratory of Professor Dr. Amar Prasad Yadav, Central Department of Chemistry T. U.) was shown in a given plot.

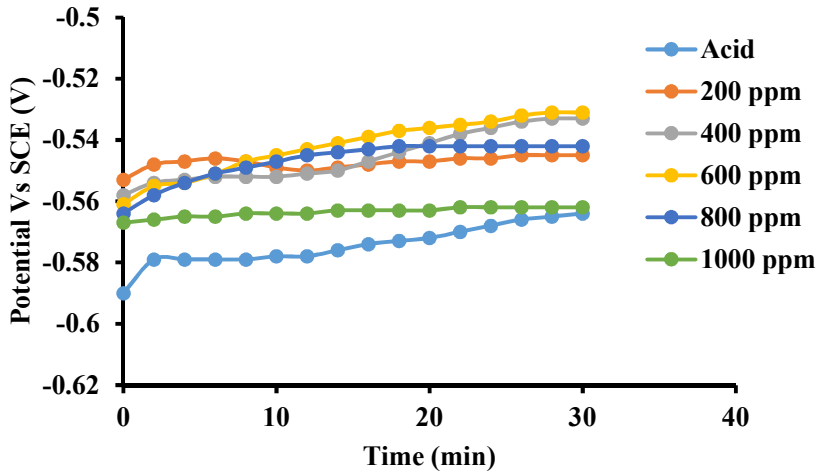

Figure 22: Variation of OCP with the time of immersion of mild steel in different concentrations of inhibitor in 1M H_2SO_4 measured at the time of immersion.

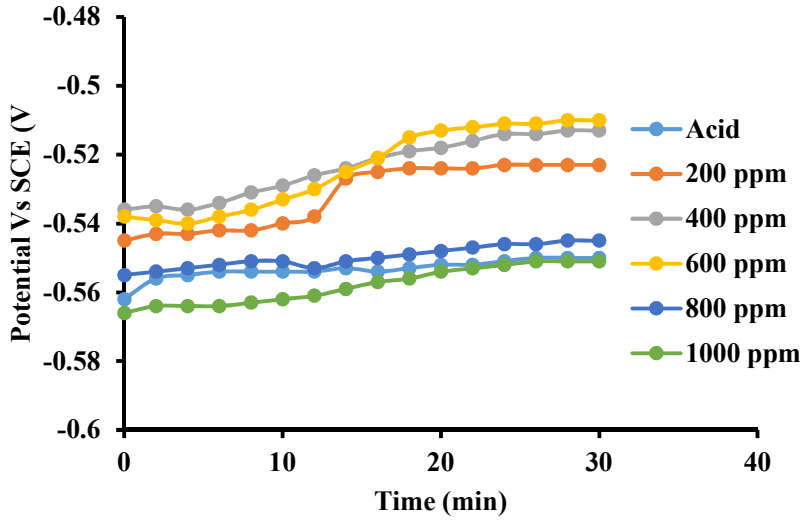

Figure 23: Variation of OCP with the time of immersion of mild steel in different concentrations of inhibitor in 1M H_2SO_4 measured after 1 h immersion in solutions.

Above figures 22 & 23 shows that initially, the potential shifted to more positive, but the shift in the value of OCP is less than 50 mV, in both immersed and as-immersed condition, indicating plant extract act as a mixed corrosion inhibitor. The shifting of potential from OCP to more positive indicates the formation of a protective layer by inhibitor molecules in acid solution on the MS surface, (i.e. Passivation) that limits the interaction of aggressive ions with the MS surface (Ijuo et al., 2016; Karki et al., 2021).

4.9.2. Polarization measurement of as-immersed MS sample in 1M H_2SO_4 and different concentrations of inhibitor solution.

The polarization of mild steel sample in acid and different concentrations of inhibitor (200, 400, 600, 800 &1000 ppm) were done by applying 300 mV in both anodic and cathodic directions by using a potentiostat. From the data of polarization of the as-immersed sample.

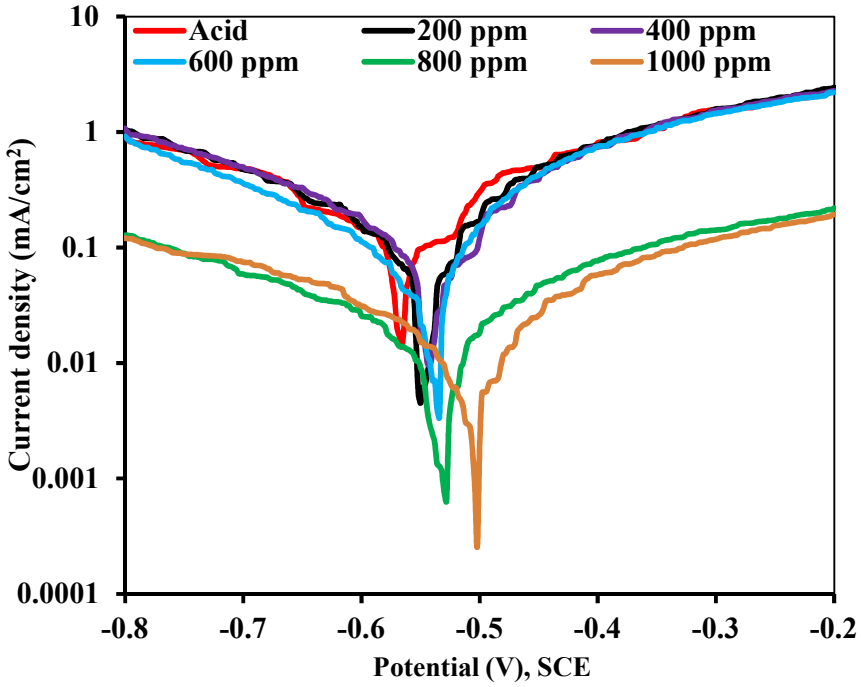

Figure 24: Potentiodynamic polarization curves for mild steel in 1M H_2SO_4 containing different concentrations of inhibitor as-immersed condition.

It is found that the anodic slope is higher than the cathodic slope for all concentrations of inhibitor as well in acid solution. This difference in slope in these half-reactions indicates, that the rate of anodic and cathodic reactions are different. The higher rate

of anodic reaction indicates that the dissolution of MS is more than the rate of hydrogen evolution reaction (HER). It is because during reaction iron metal oxidizes to a ferrous ion with the release of two electrons but the hydrogen ion accepts one electron in cathodic reaction. The Evans diagram and Tafel extrapolation indicate that the decrease in current density on the addition of inhibitor means, the MS surface is covered with inhibitor molecules so that the active site of MS is small for the reaction.

This polarization measurement of MS was carried out at a laboratory temperature of 27 ºC and the obtained results were tabulated in table 10. The result of the decrease in the corrosion current in presence of an inhibitor indicates the blockage of reacting sites by inhibitor molecules.

Table 10: Anodic and cathodic slope and inhibition efficiency for as-immersed sample.

Medium	OCP	Icorr	Anodic slope	Cathodic slope	Efficiency (%)
Acid	0.568	0.102	10.96	4.02	-
200 ppm	0.55	0.073	16.46	7.76	28.4314
400 ppm	-0.548	0.063	15.34	6.18	38.2353
600 ppm	-0.528	0.03	10.18	10.02	70.5882
800 ppm	-0.548	0.0094	8.56	4.49	90.7843
1000 ppm	-0.502	0.0064	9.22	6.25	93.7255

4.9.3. Polarization measurement of 1h-immersed MS sample

After immersion of MS coupons in different solutions at 1 h. polarization measurements were carried out at laboratory temperature (27 ºC) at a potential window ($\pm 300\ mV$). The results show starting from acid solution to acidic solution to inhibitor 1000 ppm solution, the current density found to be decreased, it is due to the resistance of inhibitor solution toward corrosion reaction. Hence like in the as-immersed condition, the current density decrease is due to coverage of MS surface by inhibitor molecules.

The inhibitor efficiency, cathodic and anodic slope, OCP and corrosion current densities obtained by potentiodynamic polarization measurement of MS in 1 h immersed condition were tabulated in table 11. Here increasing the anodic slope and decreasing the cathodic slope of the reaction with increasing the concentration of inhibitor indicates, that the inhibitor molecules block the cathodic actives sites more frequently than that of the anodic reaction.

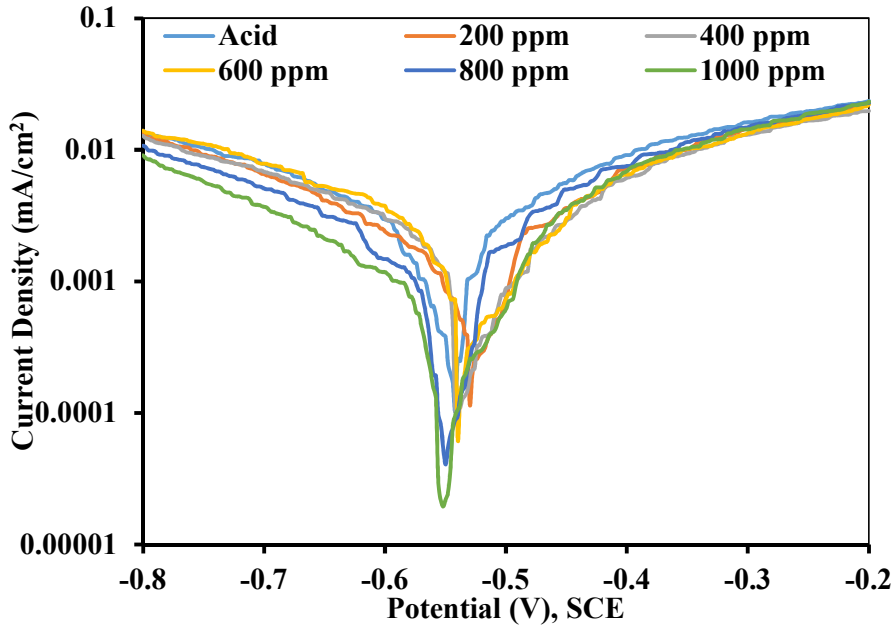

Figure 25: Potentiodynamic polarization curves for mild steel in 1M H_2SO_4 containing different concentrations of inhibitor immersed condition.

Table 11: Table showing the anodic and cathodic slope and inhibition efficiency for immersed sample.

Medium	OCP	Icorr	Anodic slope	Cathodic slope	Efficiency (%)
Acid	-0.542	0.001	6.89	5.04	-
200 ppm	-0.53	0.00088	8.75	4.89	12
400 ppm	-0.542	0.0007	12.5	4.28	30
600 ppm	-0.54	0.00054	12.59	4.2	46
800 ppm	-0.55	0.00046	10	5.09	54
1000 ppm	-0.552	0.00025	15.8	4.11	75

4.9.4 Inhibitor efficiency of methanol extract from polarization measurement

For both immersed and as-immersed samples the inhibition efficiency of the inhibitor in varying concentrations was measured by using the polarization method. The above table (Table 10 & Table 11) shows the efficiency data. The inhibition efficiency of the inhibitor is higher in the 1 hr immersed condition because at this time inhibitor molecules can have sufficient time to get adsorbed and attain an equilibrium state. The variation of efficiency of inhibitor with different concentrations for mild steel in both immersed and as-immersed conditions was shown in figure 26.

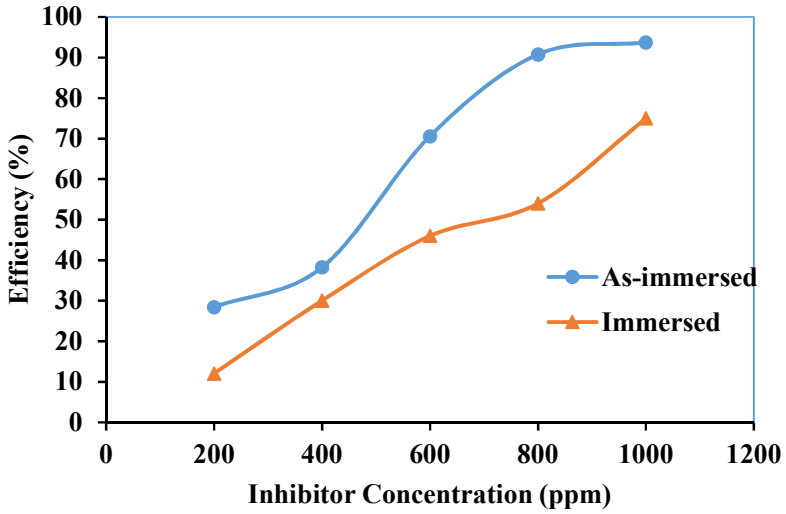

Figure 26: Inhibition efficiency of inhibitor obtained from the polarization of both immersed and as-immersed MS sample 1M H_2SO_4 in the presence and absence of inhibitor.

Figure 26 revealed that the inhibition efficiency increases with an increase in the concentration of the inhibitor solution. This is due to the increase in the fraction of surfaces covered by inhibitor molecules. The maximum efficiency was found as 93.73% and 75% at 1000 ppm concentration of the inhibitor solution in 1M H_2SO_4 on MS sample as-immersed and immersed for 1 hour respectively.

CHAPTER – 5

CONCLUSION

In this research work, a green inhibitor for mild steel in 1M H_2SO_4 was successfully prepared from bark extract of *S. Robusta*. The corrosion of mild steel was studied in the presence and absence of inhibitor by using the weight loss method and electrochemical (OCP measurement & potentiodynamic polarization) method at different concentrations (200 ppm, 400 ppm, 600 ppm, 800 ppm & 1000 ppm) of inhibitors at different periods as well at varied temperature. In the process, polyphenols are successfully extracted by methanol extract using the liquid-liquid extraction method and characterized by phytochemical and spectroscopic methods. From the data and results obtained, the following statements can be inferred,

- Alkaloids were extracted from methanol extract using the solvent extraction method. And the alkaloid yield was found very low even after several repeated experiments. So, quantitative extraction of alkaloids from the bark of *S. robusta* was not possible.
- Polyphenols were successfully extracted from the methanol fraction of bark of *S. Robusta* using the liquid-liquid extraction method and its corrosion inhibition ability was measured by using the weight loss measurement method. From weight loss data we found, as our hypothesis, it doesn't inhibit the electrochemical corrosion reaction rate. So, we can say OH- groups of polyphenol attract electrons towards themselves instead of donating the electron. Hence we conclude that polyphenols can't use as corrosion inhibitors for mild steel.
- The direct methanol extract was used as a mild steel corrosion inhibitor. The weight loss of mild steel increased with time in both the presence and absence of inhibitor in 1M H_2SO_4 which in turn increases the corrosion rate. However, the extent of weight loss is greatly reduced in presence of inhibitors. Where the weight loss of mild steel decreased with an increase in the concentration of the inhibitor in 1M H_2SO_4 and so does the corrosion rate.
- The inhibition efficiency of the inhibitor seemed to increase with the concentration of the inhibitor while decreasing with the time of immersion.

- The result of the UV spectrophotometer indicates that in the bark extract of *S. robusta*, the presence of unsaturated organic compounds has π-π* transition in the UV-visible region.
- FTIR results confirmed the presence of C-N, O-H, C-O, C=O, C-H, O-H and which act as active binding sites for adsorption.
- From the measurement of R^2 value & analysis of the adsorption isotherm, all three isotherms are not fitted.
- From the values of E_a, ΔH° and ΔS°, the decrease in entropy and increase of activation energy & enthalpy indicates the adsorption of inhibitor molecules on the MS surface or coverage of the metal surface by forming a barrier.
- The OCP measurement shows that the shifting of potential to a slightly positive direction indicates the inhibitor forming a protective layer as extract works with mixed inhibitor.
- Potentiodynamic polarization analysis showed that inhibition efficiency increased with increasing the concentration of inhibitor in both cases i.e. as-immersed and immersed for 1 hour. The maximum efficiency of the as-immersed and the immersed sample was found to be 93.73% and 75% in the 1000 ppm of inhibitor solution respectively.
- It also indicates that in the immersed sample the efficiency of the inhibitor is less than that of the as-immersed sample. It may be due to activation of reactive sites at the immersed period which continue reaction at a higher rate and it supports the weight loss data i.e. why efficiency is low in weight loss measurement and it decreases significantly with the period of immersion.

References

Ahmad, Z. (2006). *Principles of corrosion engineering and corrosion control*. Elsevier. ISBN: 9780080480336

Ali, M. M., Magee, J. C., & Hsieh, P. Y. (2020). Corrosion protection of steel pipelines with metal-polymer composite barrier liners. *Journal of Natural Gas Science and Engineering*, *81*, 103407.

Al-Shihry, S. S., Sayed, A. R., & Abd El-lateef, H. M. (2020). Design and assessment of a novel poly (urethane-semicarbazides) containing thiadiazoles on the backbone of the polymers as inhibitors for steel pipelines corrosion in CO2-saturated oilfield water. *Journal of Molecular Structure*, *1201*, 127223.

Andoor, P. A., Okeoma, K. B., & Mbamara, U. S. (2021). Adsorption and thermodynamic studies of the corrosion inhibition effect of Rosmarinus officinalis L. leaves on aluminium alloy in 0.25 M HCl and effect of an external magnetic field. *International Journal of Physical Sciences*, *16*(2), 79–95.

Aralu, C. C., Chukwuemeka-Okorie, H. O., & Akpomie, K. G. (2021). Inhibition and adsorption potentials of mild steel corrosion using methanol extract of Gongronema latifoliuim. *Applied Water Science*, *11*(2), 22. doi: 10.1007/s13201-020-01351-8

Arshad, N., Singh, A. K., Chugh, B., Akram, M., Perveen, F., Rasheed, I. and Saeed, A. (2019). Experimental, theoretical, and surface study for corrosion inhibition of mild steel in 1 M HCl by using synthetic anti-biotic derivatives. *Ionics*, *25*(10), 5057–5075.

Banu, A. M., Farzana, B. A., & Ahamed, K. R. (2021). Evaluation of inhibitive performance of Allamanda cathartica leaves extract as a green corrosion inhibitor on mild steel in acid medium. *Materials Today: Proceedings*, *47*, 2036–2047.

Baral, S., Neumann, M., Basnyat, B., Gauli, K., Gautam, S., Bhandari, S. K., & Vacik, H. (2020). Form factors of an economically valuable Sal tree (Shorea robusta) of Nepal. *Forests*, *11*(7), 754.

Berrissoul, A., Ouarhach, A., Benhiba, F., Romane, A., Zarrouk, A., Guenbour, A., and Dafali, A. (2020). Evaluation of Lavandula mairei extract as green

inhibitor for mild steel corrosion in 1 M HCl solution. Experimental and theoretical approach. *Journal of Molecular Liquids*, *313*, 113493. doi: 10.1016/j.molliq.2020.113493

Berto, F., & Fergani, O. (2017). Fatigue behaviour of welded structural steel subjected to hot-dip galvanization process. *International Journal of Fatigue*, *101*, 439–447.

Bhattarai, J. (2008). Passivation behavior of steel rod and wires of Nepal in acidic and alkaline solutions. *Nepal Journal of Science and Technology*, *9*, 157–162.

Brycki, B. E., Kowalczyk, I. H., Szulc, A., Kaczerewska, O., & Pakiet, M. (2018). Organic corrosion inhibitors. *Corrosion Inhibitors, Principles and Recent Applications*, *3*, 33.

Chapagain, A., Acharya, D., Das, A. K., Chhetri, K., Oli, H. B., & Yadav, A. P. (2022). Alkaloid of Rhynchostylis retusa as Green Inhibitor for Mild Steel Corrosion in 1 M H2SO4 Solution. *Electrochem*, *3*(2), 211–224.

Dariva, C. G., & Galio, A. F. (2014). Corrosion inhibitors–principles, mechanisms and applications. *Developments in Corrosion Protection*, *16*, 365–378.

Faraj, L., & Khan, G. M. (2015). Application of Natural Product Extracts as Green Corrosion Inhibitors for Metals and Alloys in Acid Pickling Processes-A. *Int. J. Electrochem. Sci*, *10*, 6120–6134.

Finšgar, M., & Jackson, J. (2014). Application of corrosion inhibitors for steels in acidic media for the oil and gas industry: A review. *Corrosion Science*, *86*, 17–41.

Garcia-Cabezon, C., Salvo-Comino, C., Garcia-Hernandez, C., Rodriguez-Mendez, M. L., & Martin-Pedrosa, F. (2020). Nanocomposites of conductive polymers and nanoparticles deposited on porous material as a strategy to improve its corrosion resistance. *Surface and Coatings Technology*, *403*, 126395.

Gierschner, J., Duroux, J.-L., & Trouillas, P. (2012). UV/Visible spectra of natural polyphenols: A time-dependent density functional theory study. *Food Chemistry*, *131*(1), 79–89.

Gladkikh, N., Makarychev, Y., Maleeva, M., Petrunin, M., Maksaeva, L., Rybkina, A., and Kuznetsov, Y. (2019). Synthesis of thin organic layers containing silane coupling agents and azole on the surface of mild steel. Synergism of inhibitors for corrosion protection of underground pipelines. *Progress in Organic Coatings*, *132*, 481–489.

Gupta, D. K., Awasthi, L., Das, A. K., Yadav, B., Ghimire, A., & Yadav, A. P. (2020). Corrosion Inhibition Effect of Acidic Extract of Bark of Eucalyptus Globulus on Mild Steel. *Tribhuvan University Journal*, *35*(1), 1–10.

Guruprasad, A. M., & Sachin, H. P. (2021). Novel cost-effective aqueous Amorphophallus paeoniifolius leaves extract as a green corrosion inhibitor for mild steel corrosion in hydrochloric acid medium: A detailed experimental and surface characterization studies. *Chemical Data Collections*, *34*, 100734.

Ijuo, G. A., Chahul, H. F., & Eneji, I. S. (2016). Kinetic and thermodynamic studies of corrosion inhibition of mild steel using Bridelia ferruginea extract in acidic environment. *Journal of Advanced Electrochemistry*, 107–112.

Ituen, E., Akaranta, O., & James, A. (2017a). Evaluation of performance of corrosion inhibitors using adsorption isotherm models: An overview. *Chem. Sci. Int. J*, *18*(1), 1–34.

Ituen, E., Akaranta, O., & James, A. (2017b). Evaluation of performance of corrosion inhibitors using adsorption isotherm models: An overview. *Chem. Sci. Int. J*, *18*(1), 1–34.

Kalaiselvan, A., Gokulakrishnan, K., Anand, T., Akhilesh, U., & Velavan, S. (2013). Preventive effect of shorea robusta bark extract against diethylnitrosamine-induced hepatocellular carcinoma in rats. *Int Res J Medical Sci*, *1*(1), 2–9.

Karki, N., Choudhary, Y., & Yadav, A. P. (2018). Thermodynamic, Adsorption and Corrosion Inhibition Studies of Mild Steel by Artemisia vulgaris Extract from Methanol as Green Corrosion Inhibitor in Acid Medium. *Journal of Nepal Chemical Society*, *39*, 76–85.

Karki, N., Neupane, S., Gupta, D. K., Das, A. K., Singh, S., Koju, G. M. & Yadav, A. P. (2021). Berberine isolated from Mahonia nepalensis as an eco-friendly and thermally stable corrosion inhibitor for mild steel in acid medium. *Arabian Journal of Chemistry*, *14*(12), 103423.

Kumar, S. H., & Karthikeyan, S. (2013). Amoxicillin as an efficient green corrosion inhibitor for mild steel in 1M sulphuric acid. *J. Mater. Environ. Sci*, *4*(5), 675–984.

Li, H.-J., Zhang, W., & Wu, Y.-C. (2018). Anti-corrosive properties of alkaloids on metals. In *Alkaloids-Their Importance in Nature and Human Life*. IntechOpen.

Liu, H., Wei, J., Dong, J., Chen, Y., Wu, Y., Zhou, Y. and Ke, W. (2021). Influence of cementite spheroidization on relieving the micro-galvanic effect of ferrite-

pearlite steel in acidic chloride environment. *Journal of Materials Science & Technology*, *61*, 234–246.

Makhlouf, A. S. H., & Botello, M. A. (2018). Failure of the metallic structures due to microbiologically induced corrosion and the techniques for protection. In *Handbook of Materials Failure Analysis* (pp. 1–18). Elsevier.

Mathur, N., & Chhipa, R. C. (2014). Study of Corrosion Inhibitors (Pennisetum Glaucum extracts) on Mild Steel used in Building Construction. *Inter. J. Engineer. Sci. Res. Technol*, *3*, 845.

Mauro, A. C., Ribeiro, B. D., Garrett, R., Borges, R. M., da Silva, T. U., de Paula Machado, S. and D'Elia, E. (2021). Ziziphus joazeiro Stem Bark Extract as a Green Corrosion Inhibitor for Mild Steel in Acid Medium. *Processes*, *9*(8), 1323.

Mendes, J. O., da Silva, E. C., & Rocha, A. B. (2012). On the nature of inhibition performance of imidazole on iron surface. *Corrosion Science*, *57*, 254–259.

Mohammed, A. M. (2018). UV-Visible spectrophotometric method and validation of organic compounds. *European Journal of Engineering and Technology Research*, *3*(3), 8–11.

Morozov, Y., Calado, L. M., Shakoor, R. A., Raj, R., Kahraman, R., Taryba, M. G., & Montemor, M. F. (2019). Epoxy coatings modified with a new cerium phosphate inhibitor for smart corrosion protection of steel. *Corrosion Science*, *159*, 108128.

Muthukrishnan, P., Jeyaprabha, B., & Prakash, P. (2014). Mild steel corrosion inhibition by aqueous extract of Hyptis Suaveolens leaves. *International Journal of Industrial Chemistry*, *5*(1), 1–11.

Nnanna, L. A., Uchendu, K. O., Nwosu, F. O., Ihekoronye, U., & Eti, P. E. (2014). Gmelina Arborea Bark Extracts as a Corrosion Inhibitor for mild steel in an acidic environment. *Int. J. Mater. Chem*, *4*(2), 34–39.

Oghli, H. M., Akhbari, M., Kalaki, A., & Eskandarzade, M. (2020). Design and analysis of the cathodic protection system of oil and gas pipelines, using distributed equivalent circuit model. *Journal of Natural Gas Science and Engineering*, *84*, 103701.

Peter, A., & Sharma, S. K. (2017). Use of Azadirachta indica (AZI) as green corrosion inhibitor against mild steel in acidic medium: Anti-corrosive

efficacy and adsorptive behaviour. *International Journal of Corrosion and Scale Inhibition*, *6*(2), 112–131.

Phulara, N. R. (2019). Assessment on corrosion damage of steel reinforced concrete structures of Kathmandu Valley using corrosion potential mapping method. *Journal of the Institute of Engineering*, *15*(2), 45–54.

Piccin, J. S., Dotto, G. L., & Pinto, L. A. A. (2011). Adsorption isotherms and thermochemical data of FD&C Red n 40 binding by chitosan. *Brazilian Journal of Chemical Engineering*, *28*(2), 295–304.

Rahim, M. A., Hassan, H. B., & Khalil, M. W. (1997). Naturally occurring organic substances as corrosion inhibitors for mild steel in acid medium: Concentration and temperature effects. *Materialwissenschaft Und Werkstofftechnik*, *28*(4), 198–204.

Rana, M., Joshi, S., & Bhattarai, J. (2017). Extract of different plants of Nepalese origin as green corrosion inhibitor for mild steel in 0.5 M NaCl solution. *Asian Journal of Chemistry*, *29*(5), 1130.

Revie, R. W. (2008). Corrosion and corrosion control*: An introduction to corrosion science and engineering*. John Wiley & Sons.

Salada, J.-A. T., Balala, L. M., & Vasquez, E. A. (2015). Phytochemical and antibacterial studies of Lantana camara L. leaf fraction and essential oil. *International Journal of Scientific and Research Publications*, *5*(3), 1–5.

Sayin, K., & Karakaş, D. (2013). Quantum chemical studies on the some inorganic corrosion inhibitors. *Corrosion Science*, *77*, 37–45.

Shahmoradi, A. R., Ranjbarghanei, M., Javidparvar, A. A., Guo, L., Berdimurodov, E., & Ramezanzadeh, B. (2021). Theoretical and surface/electrochemical investigations of walnut fruit green husk extract as effective inhibitor for mild-steel corrosion in 1M HCl electrolyte. *Journal of Molecular Liquids*, *338*, 116550.

Shrestha, P. R., Oli, H. B., Thapa, B., Chaudhary, Y., Gupta, D. K., Das, A. K. & Yadav, A. P. (2019). Bark extract of Lantana camara in 1M HCl as green corrosion inhibitor for mild steel. *Engineering Journal*, *23*(4), 205–211.

Shukla, S. K., & Ebenso, E. E. (2011). Corrosion inhibition, adsorption behavior and thermodynamic properties of streptomycin on mild steel in hydrochloric acid medium. *Int. J. Electrochem. Sci*, *6*(8), 3277–3291.

Silverstein, R. M., & Bassler, G. C. (1962). Spectrometric identification of organic compounds. *Journal of Chemical Education*, *39*(11), 546.

Sivakumar, P. R., & Srikanth, A. P. (2017). Anticorrosive activity of Schreabera swietenioids leaves as green inhibitor for mild steel in acidic solution. *Asian Journal of Chemistry*, *29*(2), 274–278.

Soni, R. K., Dixit, V., Irchhaiya, R., & Singh, H. (2013). A review update on Shorea robusta Gaertn f. (Sal). *Journal of Drug Delivery & Therapeutics*, *3*(6), 127–132.

Sundararajan, B., & Kumari, B. R. (2017). Novel synthesis of gold nanoparticles using Artemisia vulgaris L. leaf extract and their efficacy of larvicidal activity against dengue fever vector Aedes aegypti L. *Journal of Trace Elements in Medicine and Biology*, *43*, 187–196.

Sushma, V., Pal, S. M., & Viney, C. (2017). GC-MS Analysis of Phytocomponents in the Various Extracts of Shorea robusta Gaertn F. *International Journal of Pharmacognosy and Phytochemical Research*, *9*(6), 783–788.

Thapa, B., Gupta, D. K., & Yadav, A. P. (2019). Corrosion inhibition of bark extract of Euphorbia royleana on mild steel in 1M HCl. *Journal of Nepal Chemical Society*, *40*, 25–29.

Ugi, B. U., & Magu, T. O. (2018). Regulating localized corrosion rate of acidified ASTM A36 mild steel with Oenothera biennis extracts using thermometric and potentiodynamic polarization studies. *Carbon*, *100*, 0–25.

Umoren, S. A., Ogbobe, O., Igwe, I. O., & Ebenso, E. E. (2008). Inhibition of mild steel corrosion in acidic medium using synthetic and naturally occurring polymers and synergistic halide additives. *Corrosion Science*, *50*(7), 1998–2006.

Valet, S., Burkert, A., Ebell, G., & Babutzka, M. (2021). Determination of the corrosion product layer resistance on zinc and electrolytically galvanized steel samples by using gel electrolytes. *Electrochimica Acta*, *385*, 138191.

Verma, C., Lgaz, H., Verma, D. K., Ebenso, E. E., Bahadur, I., & Quraishi, M. A. (2018). Molecular dynamics and Monte Carlo simulations as powerful tools for study of interfacial adsorption behavior of corrosion inhibitors in aqueous phase: A review. *Journal of Molecular Liquids*, *260*, 99–120.

Wang, F., Xu, J., Xu, Y., Jiang, L., & Ma, G. (2020). A comparative investigation on cathodic protections of three sacrificial anodes on chloride-contaminated reinforced concrete. *Construction and Building Materials*, *246*, 118476.

Yahaya, L. E., Aroyeun, S. O., Ogunwolu, S. O., Jayeola, C. O., & Igbinadolor, R. O. (2017). Green and Black Tea (Camellia sinensis) Extracts as Corrosion Inhibitor for Mild Steel in Acid Medium. *World Applied Sciences Journal*, *35*(6), 985–992.

Zarras, P., & Stenger-Smith, J. D. (2014). Corrosion processes and strategies for prevention: An introduction. In *Handbook of Smart Coatings for Materials Protection* (pp. 3–28). Elsevier.

Zhang, J., Zhang, W., Wei, L., Pu, L., Liu, J., Liu, H. and Guo, Z. (2019). Alternating multilayer structural epoxy composite coating for corrosion protection of steel. *Macromolecular Materials and Engineering*, *304*(12), 1900374.